CHALMERS

Determination of acceptable contaminant levels for PEM fuel cell stacks and poisoning mitigation strategies

Master of Science Thesis in the Master Degree Program Applied Physics

AGNES ENGSTRÖM

Department of Applied Physics
CHALMERS UNIVERSITY OF TECHNOLOGY
Gothenburg, Sweden, 2014

Determination of Acceptable Contaminant Levels for PEM Fuel Cell Stacks and Poisoning Mitigation Strategies

Master of Science thesis in the Master Degree Program Applied Physics

AGNES ENGSTRÖM

Department of Applied Physics

CHALMERS UNIVERSITY OF TECHNOLOGY

Gothenburg, Sweden 2014

Determination of Acceptable Contaminant Levels for PEM Fuel Cell Stacks and Poisoning Mitigation Strategies
AGNES ENGSTRÖM

Department of Applied Physics
Chalmers University of Technology
SE-412 96 Göteborg
Sweden
Telephone +46 (0)31-772 1000

Determination of Acceptable Contaminant Levels for PEM Fuel Cell Stacks and Poisoning Mitigation Strategies

AGNES ENGSTRÖM

Department of Applied Physics
Chalmers University of Technology

Abstract

PEM fuel cells are a promising alternative to today's internal combustion engines. One problem with PEM fuel cells is performance degradation due to contaminations in the fuel. In this thesis, the acceptable contaminant levels for PEM fuel cell stacks were determined for some contaminants.

The contaminants used in this thesis were NH_3, CO, C_2H_4, C_2H_6, C_3H_6, H_2S and SO_2. The measurement methods used were electrochemical *in situ* methods. For all contaminants, the voltage was measured during contamination with different concentration levels, while the current density was held constant at 0.5 A/cm^2. For NH_3, the electrochemically active surface area and membrane resistance were measured as well. The contaminants that poisoned the fuel cells were NH_3, CO, H_2S and SO_2. For these four contaminants, the poisoning of the fuel cells was irreversible if the concentration was high enough and the exposure time long enough. The short chain hydrocarbons C_2H_4 and C_2H_6 did not show any poisoning mechanism on the fuel cells. The measurements made with C_3H_6 were not sufficient to draw any conclusions from. One poisoning mitigation strategy used to mitigate the poisoning effect of CO was the addition of small amounts of air to the fuel. The addition of 0.5 % air to the fuel increased the acceptable CO level from 10 to 25 ppm.

Keywords: PEM Fuel Cell, Degradation, Contaminations, Mitigation Strategies

Acknowledgments

I would like to express my gratitude's to Axel Bauman Ofstad and Andreas Bodén, my supervisors at PowerCell Sweden AB, and Patrik Johansson, my supervisor at Chalmers University of Technology, for their guidance during this work. I would also like to thank Istaq Ahmed for his help during my laboratory work at Volvo GTT/ATR and Yasna Acevedo Gomez for her help during my laboratory work at the Royal Institute of Technology.

Table of Contents

List of Figures

List of Tables

Tables in Appendix

List of Abbreviations

AB	Air Bleed
AC	Alternating Current
APU	Auxiliary Power Unit
CHP	Combined Heat and Power
CV	Cyclic voltammetry
DC	Direct Current
EIS	Electrochemical Impedance Spectroscopy
GDL	Gas Diffusion Layer
HFR	High Frequency Resistance
HOR	Hydrogen Oxidation Reaction
ICE	Internal Combustion Engine
KTH	Royal Institute of Technology
MEA	Membrane Electrode Assembly
MFC	Mass Flow Controller
OCV	Open Circuit Voltage
ORR	Oxygen Reduction Reaction
PAB	Pulsed Air Bleed
PEM	Proton Exchange Membrane
PSA	Pressure Swing Adsorption
PTFE	Polytetrafluoroethylene
SEHP	Sorption-Enhanced Hydrogen Production
TSA	Temperature Swing Adsorption

Chapter 1

Introduction and Basic Theory

1.1 About this Thesis

This thesis is a product of the collaboration between PowerCell Sweden AB (PowerCell), Chalmers University of Technology (Chalmers), Volvo GTT/ATR and the Royal Institute of Technology (KTH). Tests on single cell fuel cells were made at KTH. Tests on fuel cell short stacks were made at PowerCell and at Volvo GTT/ATR. The main purpose of this thesis was to investigate the poisoning effects on fuel cells of some contaminations. In addition to that, some mitigation techniques were investigated as well.

1.1.1 Limitations

In this thesis, only proton exchange membrane (PEM) fuel cells are considered. When fuel cells are mentioned, it is the PEM fuel cells that are intended, if nothing else is stated. The reasons for fuel cell degradation are several, but this thesis focuses on degradation due to impurities in the fuel. The theoretical part deals with some of the most important impurities present in reformate fuel and air. The practical measurements are made on test cells and fuel cell short stacks. The contaminants considered in these tests are NH_3, CO, C_2H_4, C_2H_6, C_3H_6, H_2S and SO_2.

1.2 Introduction

Internal combustion engines (ICE) do not have a very high efficiency in small power ranges and emit substances that are dangerous to the environment. New energy converters for vehicles are therefore needed for a sustainable energy society. One such energy converter is the proton exchange membrane (PEM) fuel cell. It converts the energy in hydrogen gas to electrical energy efficiently and with water as the only exhaust. There are however several obstacles that need to be overcome before vehicle applications of PEM fuel cells are competitive to the ICE. One such obstacle is the production and storage of hydrogen. PowerCell has developed a diesel powered fuel cell auxiliary power unit (APU). This way, the hydrogen is produced onboard which means that hydrogen storage is not needed. This could be a way to commercialize PEM fuel cells in vehicles before the hydrogen infrastructure is developed. The hydrogen produced in the APU contains impurities which result in fuel cell performance losses. The purification of the hydrogen is a costly process and it is therefore important to investigate which contaminant levels that are acceptable and how the fuel cell poisoning effects may be mitigated.

1.3 Fuel Cell Theory

There are essentially six different types of fuel cells that are viable systems at the present and the near future. These are presented in table 1.1, with the respective working temperatures, mobile ions, and applications.

Table1.1: Six types of fuel cells and their working temperatures, mobile ions, and applications.

Fuel cell type	Mobile ion	Operating temperature	Applications
Alkaline	OH^-	50-200 ˚C	Stationary and space applications
Proton exchange membrane	H^+	60-100 ˚C	Vehicles, and low power combined heat and power (CHP) systems
Direct methanol	H^+	20-90 ˚C	Portable electronic systems of low power running for long times
Phosphoric acid	H^+	~220 ˚C	200 kW CHP systems
Molten carbonate	CO_3^{2-}	~650 ˚C	Medium- to large-scale CHP systems, up to MW capacity
Solid oxide	O^{2-}	500-1000 ˚C	CHP systems with capacities from 2 kw to multi-MW

Source: [1]

In the following, only proton exchange membrane (PEM) fuel cells will be considered. PEM fuel cells are well suited for vehicle applications because they have moderate working temperatures, which promote fast start-up and, additionally, the electrolyte is non-corrosive and solid [2].

A PEM fuel cell consists of a membrane electrode assembly (MEA) with a gas diffusion layer (GDL) and bipolar plates, as illustrated in fig 1.1(a). The reactions take place in the MEA, which consists of a polymer electrolyte membrane with electrodes on both sides. The gas diffusion layer distributes the gases evenly on the cathode and anode side respectively of the MEA. The bipolar plates connect the MEAs in series and provide the gas to the cell through gas distribution channels.

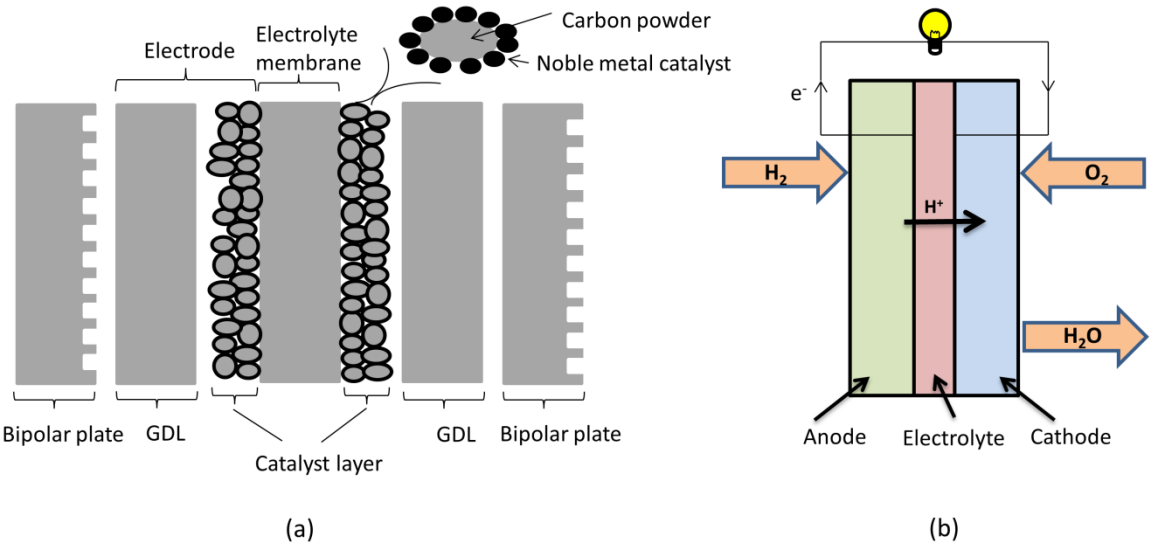

Figure 1.1: (a) A schematic picture of a PEM fuel cell (The picture is not made to scale). (b) A schematic picture of a PEM fuel cell with the gas flows.

The hydrogen gas (H_2) is supplied to the anode, where it is oxidized (HOR). The H^+ ions (protons) formed pass through the electrolyte to the cathode, while the electrons are transferred through an external circuit, as illustrated in fig 1.1(b). At the same time on the cathode side, air is supplied and

oxygen is reduced (ORR) and then reacts with protons (H^+) and electrons (e^-) to form water. These reactions are represented in the following reactions

Anode:	$2H_2 \rightarrow 4H^+ + 4e^-$	(1.1)
Cathode:	$O_2 + 4e^- + 4H^+ \rightarrow 2H_2O$	(1.2)
Total reaction:	$2H_2+O_2 \rightarrow 2H_2O$, resulting potential: 1.23 V	(1.3)

The reactions on both sides are speeded up by a catalyst, usually platinum or a platinum alloy [3].

1.3.1 Electrolyte

The electrolyte in a PEM fuel cell is a polymer. The most important properties of the electrolyte are good proton conductivity and to be electrically insulating and gas tight [1]. One such polymer is Nafion®, which was developed by DuPont [1]. Nafion® has a backbone of polytetrafluoroethylene (PTFE) with side chains terminating in a sulfonic acid group-HSO_3 [1] [3]. The hydrogen is ionic bonded to the side chain, resulting in SO_3^- at the end of the side chain and one loose H^+ ion, see fig 1.2. The side chains are attracted by each other and forms clusters. The PTFE is hydrophobic and the HSO_3 is hydrophilic, which means that Nafion® is a hydrophobic material with hydrophilic clusters. Water can be absorbed in these clusters, as illustrated in fig 1.2. When water is absorbed, the charge of the sulfonic group and proton becomes screened, and as a result the proton becomes mobile [1]. This way the Nafion® has good proton conductivity when hydrated. The hydrophobicity of the PTFE prevents the fuel cell from flooding. Other polymers used as electrolytes have similar properties as Nafion® [1].

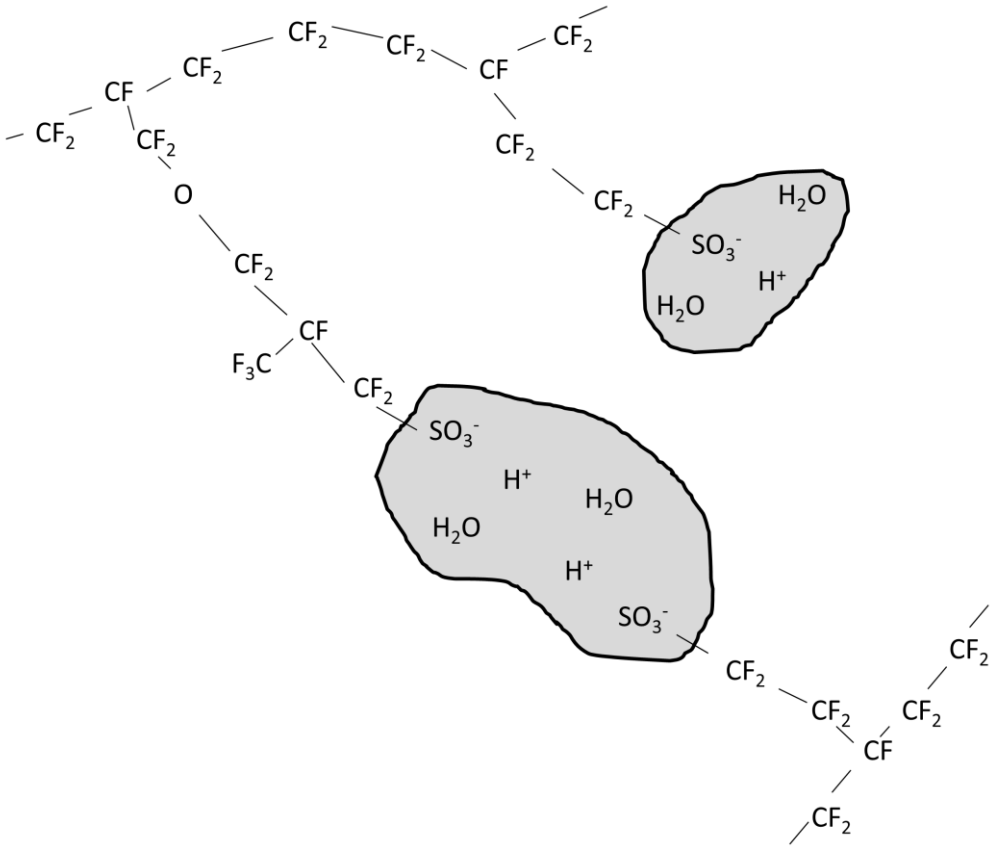

Figure 1.2: A model figure of Nafion® with hydrophilic clusters containing water molecules.

1.3.2 Electrodes

The anode and cathode electrodes are usually similar and can be identical. The catalyst (*e.g.* platinum (Pt)) is distributed on a support, e.g. carbon powder particles, as illustrated in fig 1.1(a). For CO-tolerance on the anode, a platinum/ruthenium alloy can be used as catalyst. Because the catalyst is an expensive noble metal, the catalyst particles are small (nanoscale) and distributed in a way to maximize the active surface area with a minimal amount of noble metal material. The catalyst loading can be around 0.4-0.5 mg/cm^2. The catalyst support material is either fixed directly onto the electrolyte, or onto a carbon cloth/paper that also works as the gas diffusion layer. If the carbon powder is fixed directly onto the electrolyte, the carbon cloth/paper is applied subsequently. [1] [3]

1.4 Fuel Cell Degradation

The lifetime of a PEM fuel cell is limited due to degradation. Membrane, catalyst layer, GDL, and bipolar plates are all parts of the fuel cell that may degrade during operation [4].

The main reasons for membrane failure are chemical degradation, mechanical degradation and short circuiting. Chemical degradation is caused by radical species formed as by-products or side reactions of the fuel cell electrochemical reactions. Mechanical degradation is when the membrane is fractured because of stress caused by humidity and thermal fluctuations. Short circuiting is when an electric current passes through the membrane which can be caused by cell over-compression and topographical irregularities. [4]

When the catalyst particle sizes increase, the catalytically active surface area decreases, leading to fuel cell performance degradation. The reasons for catalyst particle growth are minimization of the clusters' surface energy, agglomeration of Pt particles on carbon support due to random cluster-cluster collisions, and the dissolution of small Pt particles in the ionomer phase, which redeposit on the surface of large particles [5]. Mayrhofer *et al.* [6] found in a study of fuel cell catalyst degradation that the Pt particles may also detach from the support and dissolve into the electrolyte. The catalytically active surface area may also decrease by adsorption of contaminants on Pt nanoparticle sites [4].

The two main GDL degradation mechanisms are changes in the structure of the GDL due to carbon corrosion and mechanical stress and wetting behavior changes due to loss of the hydrophobic agent and carbon surface changes.

Bipolar plates made of corrosion-resistant metals forms an oxide layer on the surface, which increases the contact resistance. This degradation problem can be avoided with bipolar plates made of graphite composites. The composite needs to have a high carbon to polymer ratio to have low interfacial contact resistance and high electrical conductivity. The high carbon ratio will however make the composite brittle. [4]

1.5 Methods for Analyzing Fuel Cell Degradation

To optimize the fuel cell system, the reasons for a decrease in performance need to be known, and consequently, methods for analyzing fuel cell degradation are needed. Some of these methods are presented below.

1.5.1 Open Circuit Voltage

The open circuit voltage (OCV) of a fuel cell is the difference in potential between the anode and cathode side at zero current. The theoretical OCV can be calculated using the difference between the Gibbs free energy for the reactants and the product. For a H_2/air fuel cell with liquid water as the product, at 25 ˚C and 1 atm pressure, the difference in Gibbs free energy is -237 kJ/mol. This gives a theoretical OCV of 1.23 V. If the product is water vapor, the Gibbs free energy is instead -229 kJ/mol, which results in the theoretical OCV of 1.19 V [7]. The theoretical OCV will increase with an increase in hydrogen and oxygen pressure, and decrease with higher temperatures. The theoretical OCV can be calculated with the Nernst equation [8]. The Nernst equation for the PEM fuel cell reaction has the form of eq 1.4.

$$E = E^0 - \frac{RT}{2F} ln\left(\frac{1}{P_{H_2}\sqrt{P_{O_2}}}\right), \quad (1.4)$$

where E is the theoretical OCV, E^0 is the equilibrium voltage with all species at their standard states, R is the gas constant, T is the absolute temperature, F is the Faraday constant and P_i is the partial pressure, in atmospheres, with the standard state being P=1 atm [8]. The measured OCV is always lower than the theoretical value. One reason for this is hydrogen crossover from the anode to the cathode side [7].

1.5.2 Polarization Curves

A polarization curve shows how the voltage changes with the current density. From this curve the maximum power output can be calculated with eq 1.5.

$$P = U * I \quad (1.5)$$

From eq 1.4 it is clear that the maximum power output is obtained if the voltage stays high as the current is increased. Figure 1.3 shows a typical polarization curve for a PEM fuel cell and the corresponding power output.

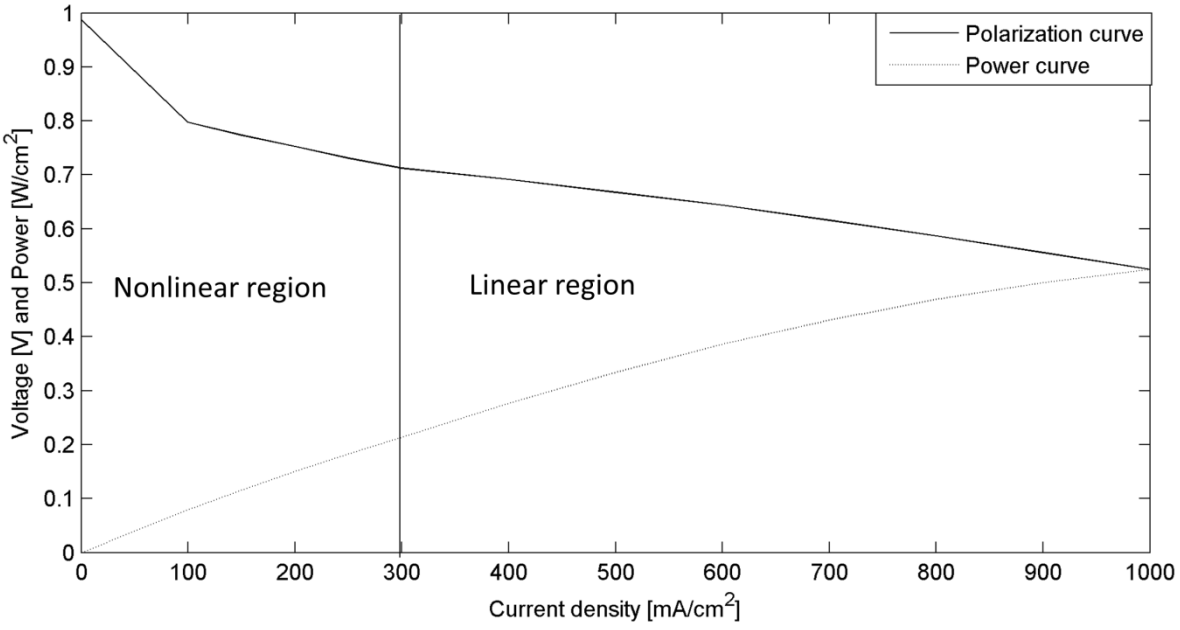

Figure 1.3: A polarization curve and the corresponding power curve.

As the current density is increased from zero, the voltage drops at first rapidly and nonlinearly. This is called the activation overpotential and is a result of internal fuel crossover and losses for the HOR and ORR. As the current density is increased further, the voltage drop becomes more linear. This is called the ohmic overpotential. This loss is due to the electrical resistance in the electrodes and the interconnections, and the ionic resistance in the electrolyte. At high current density (not shown in fig 1.3), the voltage drops rapidly again due to a decrease in fuel concentration at the electrode surface, which is why this loss is called the concentration overpotential or mass transport loss. [1]

The activation losses can be expressed as

$$\eta_{act} = a + b\log I, \tag{1.6}$$

where *a* and *b* are constants. This is called the Tafel equation [1]. The activation losses are thus linearly dependent on the logarithm of the current density.

1.5.3 Electrochemical Impedance Spectroscopy

With electrochemical impedance spectroscopy (EIS), information such as electrolyte resistance, adsorption of electro active species, charge transfer at the electrode surface and mass transfer from the bulk solution to the electrode surface, can be extracted. To do this, the system is considered to be an electrical circuit where each component (or segment of simple electric circuit) represents one of the electrochemical processes.

When performing impedance spectroscopy, an AC current is added to a constant DC signal. The amplitude of the AC current needs to be small enough to be able to approximate the system to be linear [9]. The AC signal is scanned over a range of frequencies and the impedance change is recorded. The scanning range should be as wide as possible, at least 6 to 7 decades, for example from 10^{-2} Hz to 10^{5} Hz [9].

For a fuel cell running at OCV, the mass transfer resistance is negligible and the impedance ($Z(\omega)$) is given by eq 1.7.

$$Z(\omega) = R_m + \frac{R_{ct}}{1+\omega^2 R_{ct}^2 C_{ct}^2} - \frac{j\omega R_{ct}^2 C_{ct}}{1+\omega^2 R_{ct}^2 C_{ct}^2}, \tag{1.7}$$

where R_m is the membrane resistance, R_{ct} is the charge-transfer resistance, C_{ct} is the charge transfer related capacity and ω is the AC frequency. From eq 1.7 it can be seen that high frequencies result in an impedance almost equal to R_m. At low frequencies, the impedance is the sum of R_m and R_{ct}. The impedance can be illustrated in a Nyquist plot, as in fig 1.4, where the imaginary part of the impedance is plotted as a function of the real part of the impedance. The product of R_{ct} and C_{ct} can be calculated from the frequency yielding the maximum imaginary impedance. This way, all the parameters in eq 1.7 can be calculated from the AC impedance spectrum. [7]

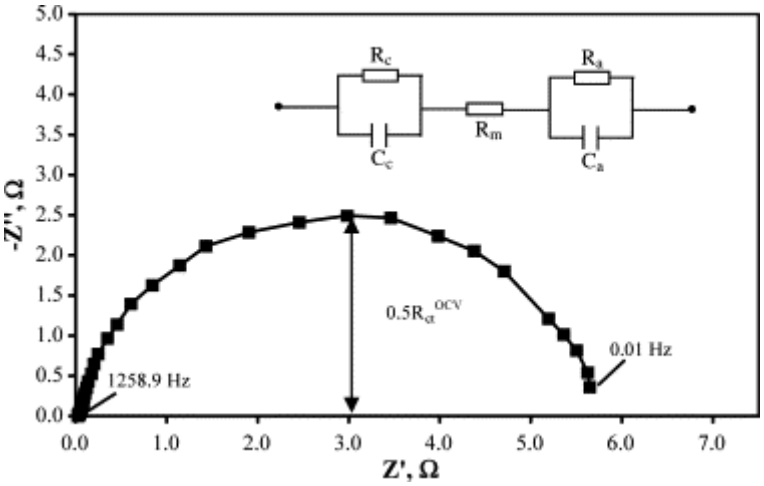

Figure 1.4: A Nyquist plot for a fuel cell working at OCV, 80˚C, 3 atm, and 100 % relative humidity. Reproduced from [10] with permission.

1.5.4 Cyclic Voltammetry

With cyclic voltammetry (CV), information about electrochemical reactions such as kinetics, thermodynamics and reversibility, can be received. With this method, the potential of a working electrode is scanned linearly in cycles, from a starting value up to a final value and back again. In these cycles, the response current is recorded and plotted against the potential in a cyclic voltammogram, as in fig 1.5. If it is assumed that a redox species exists only in oxidized form from the start of the cycle, there will be no response current at first. As the potential approaches the Nernst potential, a reduction current will start to flow. The reduction current will increase with the potential until it reaches a peak where the reaction speed is determined by the mass transfer rate of oxidized form to the electrode surface and will then decrease. The decrease in reduction current is due to the increase in thickness of the diffusion layer near the electrode surface. When the scanning of the potential is reversed, the species that were reduced in the forward scanning are oxidized back to the oxidized form. Once again there will be a peak and then a decline in the current. [7]

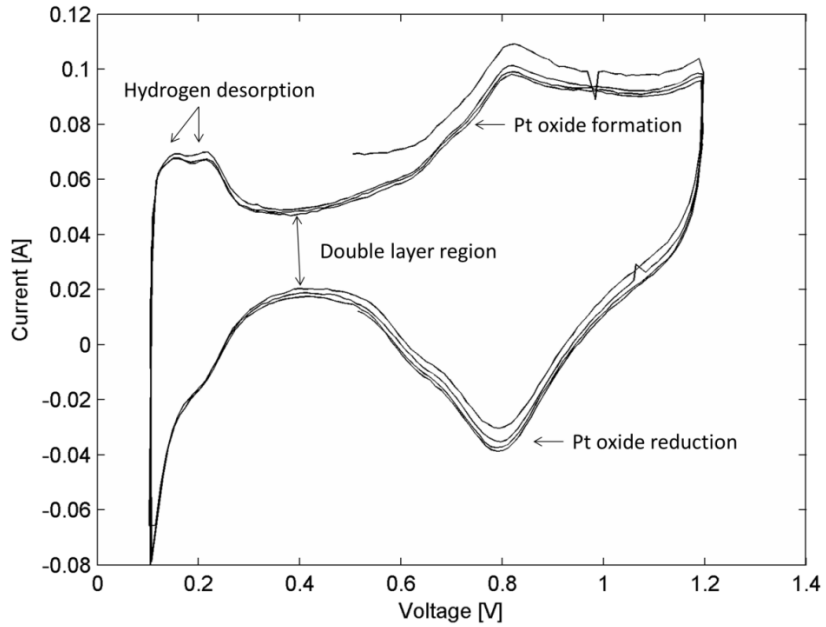

Figure 1.5: A cyclic voltammetry made with the scanning rate 50 mV/s, cycled three times.

For a reversible redox process the peak current is proportional to $v^{1/2}$, where v is the potential scanning rate, and the reduction current peak is the same size as the oxidation current peak. Other characteristics for a reversible redox process are that the position of the peak does not change with the scanning rate and that the separation between the position of the anodic and cathodic peak ($E_{p,a}$ and $E_{p,c}$) is given by the constant ΔE_p:

$$\Delta E_p = E_{p,a} - E_{p,c} = 2.3\frac{RT}{nF} = \frac{0.059}{n}\text{ V (at 25 ˚C)}, \quad (1.8)$$

where n is the number of electrons in the reaction. This way the electron number can be obtained from the voltammogram. The peak current, i_p, is given by:

$$i_p = (2.69 * 10^5)n^{3/2}AD_0^{1/2}C_0v^{1/2}, \quad (1.9)$$

where A is the electrode area given in cm^2, D_0 is the diffusion coefficient of the oxidized form of the redox species in cm^2/s, C_0 is the concentration of the oxidized form in the solution in mol/cm^3 and v is given in V/s. With eq 1.9, the diffusion coefficient, electrode area, and the electro active species concentration can also be obtained from the voltammogram. To obtain the thermoelectric potential of the redox reaction, the anodic peak potential and the cathodic peak potential are averaged. For a reversible process, the reactions are very fast so the kinetic parameters cannot be obtained. [7]

In the irreversible case the peak current is given by the equation:

$$i_p = (2.69 * 10^5)n(\alpha n_a^{1/2})AD_0^{1/2}C_0v^{1/2}, \quad (1.10)$$

where α is called the charge transfer coefficient and n_a is the electron number involved in the charge transfer. As seen from the eq 1.10, the peak current is once again proportional to $v^{1/2}$, but it is smaller than the value for the reversible case. With the equation for the separation between the peak potential and the half-wave potential ($E_{p/2}$), the value of αn_a can be obtained:

$$|E_p - E_{\frac{p}{2}}| = \frac{1.857RT}{\alpha n_a}\text{ mV at 25 ˚C. [7]} \quad (1.11)$$

Cyclic voltammetry can be used in a way to easily obtain the electrochemically active area of platinum in a fuel cell. When the cathode is investigated, it is exposed to nitrogen gas and the anode side is exposed to hydrogen. The potential is cycled between 0 and 1.2 V (0-0.7 V if the catalyst is a Pt alloy containing ruthenium (Ru)). The total hydrogen adsorbed onto platinum can be obtained by integrating over the hydrogen desorption peak. The electrochemical active Pt area is calculated assuming that the hydrogen is adsorbed in a monolayer. To convert from Coulomb, which is received from the integration to cm^2, a specific capacitance of 210 μC/cm^2 of Pt for the hydrogen desorption reaction can be used. [11]

1.5.5 Carbon Monoxide Stripping

CO stripping can be used to determine the electrochemically active surface area in a fuel cell. This area is the surface area of the metal particles in the electrodes that are in contact with the electrolyte and the current collector at the same time. CO stripping is useful when investigating the catalyst durability in a PEM fuel cell. The surface area of the catalyst is not given as an absolute value, but rather as a relative [12]. The measurement consists of three parts and can be performed like this: first a cyclic voltammetry without N_2 flow, then potentiostatic holding at 0.100 V while CO is

being adsorbed on the catalyst surface for 15 minutes, followed by a cleaning out with N_2 for 45 minutes. Finally the CO is stripped by cyclic voltammetry.

1.5.6 Hydrogen Crossover Analysis

In a low temperature fuel cell, the hydrogen crossover affects the OCV so the measured value is distinctly lower than the theoretical value. Hydrogen crossover is when one hydrogen molecule passes through the electrolyte, from anode to cathode, where it reacts with oxygen. This way two electrons are passing through the electrolyte, instead of passing through the external circuit, which is called internal current. The hydrogen crossover and internal current can therefore be considered as equivalent. With an internal current, the current at OCV is not zero. The voltage of a fuel cell without an internal current can, for low current densities (i), be approximated by the equation:

$$V = E - Aln\left(\frac{i}{i_0}\right), \tag{1.12}$$

with the constants $E = 1.2$ V, $A = 0.6$ V, $i_0 = 0.04$ mAcm^{-2}. Equation 1.12 is valid for small current densities because it only takes the activation losses into account. With fuel crossover, and thus an internal current (i_n), the equation can be rewritten as:

$$V = E - Aln\left(\frac{i+i_n}{i_0}\right). \tag{1.13}$$

For a low temperature fuel cell, a typical value of i_n is 3 mAcm^{-2}. [1]

Linear sweep voltammetry can be used to measure the hydrogen crossover. With this method, nitrogen gas is supplied to one side of the fuel cell and hydrogen gas to the other side. The voltage is swept from 0 V to around 0.5 V, with a sweeping rate of around 4 mV/s. Figure 1.6 shows a linear sweep voltammetry plot. At first, the current increases with increasing voltage, and then it levels off due to a limiting rate of hydrogen crossover at higher voltages. In fig 1.6, the current never levels off completely due to some short circuiting in the cell. The total hydrogen crossover (given in moles per second) can be obtained from the maximum current (I_{max}) with the following equation:

$$N_{H_2} = \frac{I_{max}}{2F}, \tag{1.14}$$

where *F* is the Faraday constant. [11]

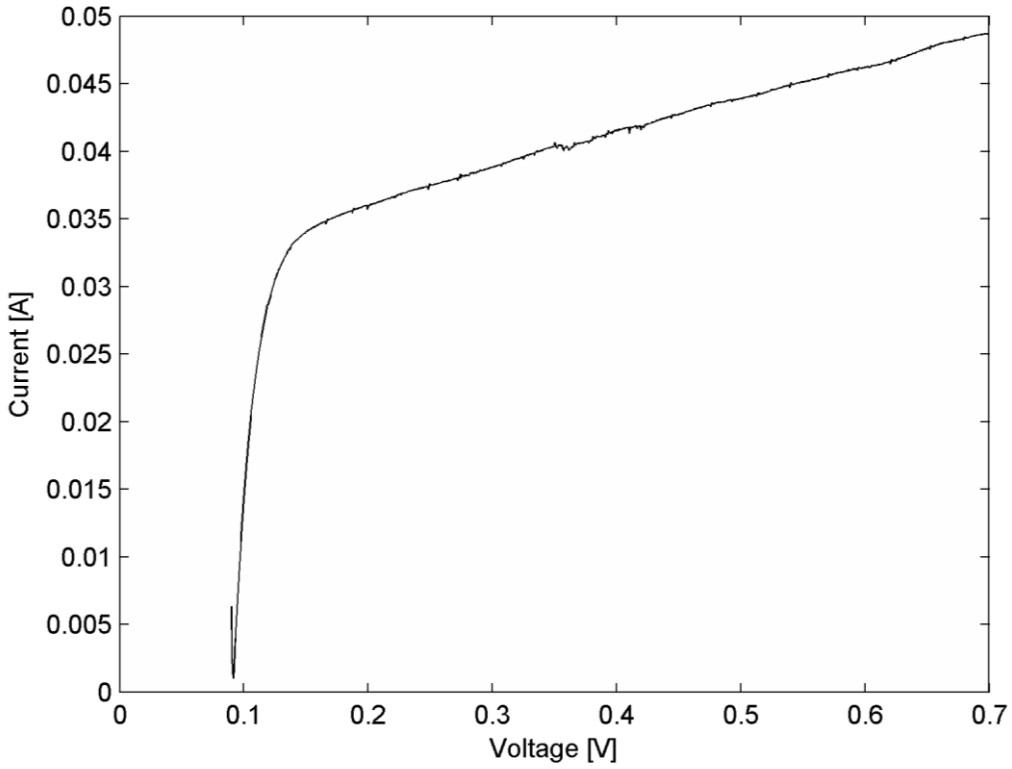

Figure 1.6: Linear sweep voltammetry.

The presence of hydrogen crossover can also be seen in a cyclic voltammogram. If the double layer region is not centered around zero current, there is hydrogen crossover.

1.6 Hydrogen Production

Hydrogen can be produced in processes generating hydrogen from carbon-based raw materials or by generating hydrogen from water. Hydrogen production from water is a carbon-neutral process, which is a great advantage. The disadvantage is that it is a difficult process that needs addition of a lot of energy. Hydrogen generation from carbon-based raw materials can be divided into three main technologies; reforming reactions, decomposition reactions, and partial oxidation reactions. Reforming reactions and decomposition reactions are highly endothermic processes, which mean that thermal heat needs to be added to the systems. The partial oxidation reaction is not endothermic. When a fraction of the fuel is oxidized, thermal energy is released, which provides energy for the main process. The process is called autothermal if the energy released in the oxidation process is equal to the energy needed for the hydrogen production. The major hydrogen production processes are listed in table 1.2. [8]

Table 1.2: Hydrogen production technologies.

Process	Reaction	ΔH^0_{298} (kJ/mol)
Reforming processes		
Steam reforming of natural gas	$CH_4+H_2O \rightarrow CO+3H_2$	206
Steam reforming of coal	$CH_xO_y+(1-y)H_2O \rightarrow (0.5x+1-y)H_2+CO$	
Steam reforming of biomass	$C_nH_mO_z+2(n-z)H_2O \rightarrow nCO+(n+0.5m-z)H_2$	
Steam reforming hydrocarbons	$C_nH_m+nH_2O \rightarrow nCO+0.5(m+2n)H_2$	49
Steam reforming of oxygenated hydrocarbon	$CH_3OH + H_2O \rightarrow CO_2 + 3H_2$	49.4
Carbon dioxide reforming of methane	$CH_4 + CO_2 \rightarrow 2CO + 2H_2$	247.3
Hydrogen sulfide reforming of methane	$CH_4 + 2H_2S \rightarrow CS_2 + 4H_2$	233
Decomposition processes		
Methane decomposition (pyrolysis)	$CH_4 \rightarrow C + 2H_2$	75.6
Water decomposition	$H_2O \rightarrow 0.5O_2 + H_2$	285.8
Hydrogen sulfide decomposition	$H_2S \rightarrow 0.5S_2 + H_2$	79.9
Partial oxidation & autothermal processes		
Methane partial oxidation	$CH_4 + 0.5O_2 \rightarrow CO + 2H_2$	-36
Autothermal steam reforming of methane	$CH_4 + xO_2 + yH_2O \rightarrow (0.5x + y)\ CO + 3H_2$	-192
Methanol partial oxidation	$CH_3OH + 0.5O_2 \rightarrow CO_2 + 2H_2$	-192.2
Coal gasification	$C + xO_2 \rightarrow CO$	
Biomass gasification	$C_nH_mO_z + 0.5(n - z)O_2 \rightarrow nCO + 0.5mH_2$	
Biomass autothermal reforming	$C_nH_mO_z + yO_2 + 2(n - y - 0.5z)H_2O \rightarrow nCO_2 + 2(n - y - 0.5z + 0.25m)H_2$	

Source: [8]

1.7 Contaminants

The contaminations in a fuel cell system originate from the fuel, the air and the different components in the fuel cell stack. These contaminants affect different parts of the cell, *e.g.* the anode, the electrolyte membrane, and the cathode. Table 1.3 shows the different contaminants present in the hydrogen gas when produced from different fuels.

Table 1.3: Possible contaminants in hydrogen gas from different fuels.

Fuel for hydrogen gas	Contaminants
Gasoline, diesel	CO, NH_3, H_2S, HCN, hydrocarbons, aldehydes, mercaptans
Natural gas	CO, NH_3, H_2S, HCN, hydrocarbons, mercaptans
Methanol	CO, odorants, alcohols
Biomass	cations, aldehydes, alcohols, formic acid, NH_3, H_2S, HCN,
Water electrolysis	Anions, cations

Source: [8]

In the following sections, some contaminants usually present in the reformate from diesel, and how these affect the fuel cell performance, will be presented. Finally, nitrogen oxides and sulfur dioxide will be presented as air contaminants on the cathode side of the fuel cell.

1.7.1 Carbon Monoxide

Carbon monoxide (CO) is one of the most investigated contaminants in reformate fuels. The CO reduces the active surface area by occupying the Pt sites because the CO-Pt bond is much stronger than the H-Pt bond [8]. When the CO-Pt bond is formed, the fuel cell efficiency is decreased further because the reactivity of the remaining unoccupied sites is decreased through dipole interactions and electron capture [8].

The CO can be adsorbed onto bare Pt sites as well as Pt hydride sites [13] [14]. The adsorption is expressed in the following chemisorption reactions:

$$CO + Pt \rightarrow Pt\text{-}CO_{ads} \quad (1.15)$$

$$2CO + 2Pt\text{-}H_{ads} \rightarrow 2Pt\text{-}CO_{ads} + H_2 \quad (1.16)$$

The bond between CO and Pt can be either linear or bridged. As illustrated in fig 1.7, when one CO molecule occupies one Pt site the mode is linear, while when bridged one CO molecule occupies two Pt sites.

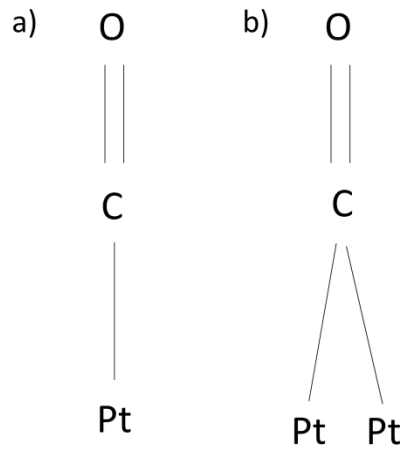

Figure 1.7: CO-Pt bonds; a) linear mode, b) bridge mode.

The effect of the CO poisoning depends on the temperature, the concentration of CO, the exposure time to CO, and the catalyst type [14]. An increase in temperature decreases the CO poisoning effect because of the enhanced hydrogen electro-oxidation and CO desorption [14]. An increased temperature is, however, only possible with an improved membrane [14]. The CO desorption is described in reaction 1.17 and 1.18.

$$Pt + H_2O \rightarrow Pt\text{-}OH_{ads} + H^+ + e^- \quad (1.17)$$

$$Pt\text{-}CO_{ads} + Pt\text{-}OH_{ads} \rightarrow 2Pt + CO_2 + H^+ + e^- \quad (1.18)$$

The poisoning phenomena of CO increases with increasing concentration and concentrations of only a few ppm can cause significant loss in fuel cell efficiency. The poisoning effect is more severe at high current densities [8]. Results from an investigation, where a gas mixture of reformate with CO was compared to a mixture of pure hydrogen with CO, show that CO poisoning is more sever when reformate fuel is utilized. This means that the relative concentration of CO to H_2 affects the severity of the poisoning phenomena [14]. An increased exposure time to CO increases the effects of the CO poisoning [8].

An increase in pressure increases the concentration of hydrogen more than that of CO, which mitigates the poisoning phenomena. The effect is small however because the probability of CO sticking on Pt is 15 times higher than that of hydrogen [14].

1.7.2 Carbon Dioxide

With carbon dioxide (CO_2) in the fuel, a fuel cell performance loss has been observed, especially at high current densities and low temperatures [8] [13]. The main reason for the performance loss is that CO_2 can be catalytically converted into CO, which in turn poisons the catalyst [8]. The CO can be produced through the following reactions:

$$2Pt + H_2 \rightarrow 2Pt\text{-}H_{ads} \quad (1.19)$$

$$CO_2 + 2Pt\text{-}H_{ads} \rightarrow Pt\text{-}CO_{ads} + H_2O + Pt \quad (1.20)$$

One experiment showed that only 1 % CO_2 in the fuel can lead to enough CO to poison more than 50 % of the Pt sites [13]. Another study showed that the effect of CO_2 reduction was very small if the fuel already contained small amounts of CO [13]. Another reason for the loss in fuel cell performance can be the decrease in H_2 partial pressure, in the presence of CO_2 [8].

1.7.3 Hydrogen Sulfide

Very small amounts of hydrogen sulfide (H_2S) can cause significant fuel cell performance drop [8] [13]. One experiment showed that 5 ppm H_2S in H_2 resulted in a 96 % drop in fuel cell performance at 50 ˚C within 12 hours [8]. The H_2S poisons the cell by adsorbing dissociatively onto the Pt. The S-Pt bond is very strong, which makes it difficult for the fuel cell to recover with pure H_2 alone. For the fuel cell to recover, a potential higher than 0.9 V above the zero potential is needed as well [8]. The adsorbed sulfur is then oxidized through the following reactions:

$$Pt\text{-}S + 3H_2O \rightarrow SO_3 + 6H^+ + 6e^- + Pt \quad (1.21)$$

$$Pt\text{-}S + 4H_2O \rightarrow SO_4^{2-} + 8H^+ + 6e^- + Pt \quad (1.22)$$

Similar to CO, the H_2S poisoning phenomena becomes more severe with increased concentration, exposure time and current density, as well as decreasing temperature [8].

1.7.4 Ammonia

Ammonia may be present both in the hydrogen fuel and in the ambient air. It is probably not important whether the ammonia enters on the anode or on the cathode side of the fuel cell because the diffusion of ammonia from one side to the other is fast [15]. The presence of small amounts of ammonia (NH_3) in the fuel decreases the fuel cell efficiency; experiments have shown that even 1 ppm NH_3 in the fuel is harmful for the fuel cell [16]. The poisoning effect can be both reversible and irreversible, depending on the concentration of NH_3 and the exposure time [13] [17]. An experiment with cyclic voltammetry of the anode did not show any noticeable adsorption of NH_3 onto the catalyst [17]. The NH_3 instead decreases the ionic conductivity of the membrane by replacing the H^+ ions with NH_4^+. If all H^+ ions are replaced by NH_4^+ ions in a Nafion® membrane, the conductivity will decrease to about one quarter of its originating value [8]. However, the decrease in ionic conductivity only explains part of the fuel cell performance loss [16]. The presence of NH_3 may affect both the HOR on the anode and the ORR on the cathode. At low current densities the effect of NH_3 on the HOR is small and the effect on the ORR is of most importance. At high current densities however, the effect of ammonia on the HOR is also important but it is not clear how the NH_3 affects the HOR [16]. The presence of ammonia may affect both the activity and the selectivity of the ORR. The desired selectivity of the ORR is the four-electron pathway to H_2O and the undesired is the two-electron pathway to H_2O_2, as in eq 1.23. [15].

$$O_2 + 2H^+ + 2e^- \rightarrow H_2O_2 \qquad (1.23)$$

When Zhang *et al.* [18] examined ammonia contamination with cyclic voltammetry and EIS they found evidence that NH_3 can contaminate both catalyst layer and the membrane. They found that the contamination of the electrodes can be fully recovered, while the recovery of the membrane is slower. They concluded that the active area of the catalyst may be decreased by adsorbents formed on Pt surface. They also showed that the recovery of the electrodes could be improved by decreased cell potential due to potential oxidation of NH_3 and the adsorbents NH_3 forms on the surface of the cathode electrode. When Zhang *et al.* [18] performed CVs; ammonia was continuously supplied to the anode. This could be a reason why they, in difference from earlier measurements [17], found some poisoning of the catalyst using CV. If the ammonia is supplied during operation of the cell, the cell must be purged with pure gases before any CV can be made and during this purge, the NH_3 may be removed.

1.7.5 Hydrocarbons

Hydrocarbons are usually present in the reformate. Methane is the most common hydrocarbon impurity and has no known poisoning effect on the fuel cell [17]. Kortsdottir *et al.* [19] examined the effect of low concentrations of ethane (100 ppm) in the hydrogen feed. They found no significant voltage loss in a fuel cell running on hydrogen and oxygen at a constant load at 80 ˚C and high humidity. No article was found on ethylene contamination in fuel cells. When a study was performed to investigate the influence of propene impurities on the PEM fuel cell catalyst [20], it was detected that the propene adsorbed onto the catalyst. When a small amount of hydrogen gas was mixed with the propene as the carrier gas, there was a decrease in the amount of adsorbed impurities. This

means that the adsorption of propene on the catalyst may not be a problem in fuel cell applications since hydrogen is then present in the anode gas.

1.7.6 Nitrogen Oxides

Nitrogen oxides (NO_x) exist in air mainly as NO_2 and NO. About 80 % of the NO_x is NO_2 and about 20 % is NO [21]. The environmental aim for NO_2 level in Sweden is 0.017 ppm, which also is about the measured values in the larger cities [22]. The level of NO_2 along a busy road can however be much higher [22]. Fenning *et al.* [21] performed experiments on a fuel cell with air contaminated with 1 ppm NO_2. After 100 hours with the contaminated air, the potential of the cell had decreased from 0.67 V to 0.60 V. The fuel cell potential went up to 0.64 V after running on pure air and after CV scanning. In the CV scan they could see an oxidation peak indicating that the degradation of the cell performance was related to the adsorption of NO_2 on the catalyst layer. The oxidation of the adsorbed NO_2 can be described by eq 1.24, which has the standard electrode potential 0.80 V, agreeing with the CV curves.

$$NO_2 + H_2O \rightarrow NO_3^- + 2H^+ + e^- \quad (1.24)$$

They concluded that small amounts of NO_2 give small fuel cell performance losses that are almost fully recoverable [21].

Daijun *et al.* [23] performed tests on a fuel cell with air contaminated with NO and NO_2 with a ratio of 9:1. When the test was performed with 1480 ppm NO_x the fuel cell voltage dropped from 0.67 V to 0.37 V within 5 minutes and finally stabilized at 0.34 V. When the NO_x was shut off, the voltage increased to 0.48 V within 3 minutes and then slowly increased to 0.60 V. Complete recovery was obtained after purge with N_2 overnight. They concluded that the fuel cell performance was almost fully recoverable after exposure to NO_x, but the recovery took a very long time and they could see a small permanent change in impedance. They suggested that the NO_x reactions taking place at the cathode were reaction 1.25 and 1.26.

$$2NO + O_2 \rightarrow 2NO_2 \quad (1.25)$$

$$2NO_2 + H_2O \rightarrow HNO_3 + HNO_2 \quad (1.26)$$

The nitrous acid (HNO_2) could then be converted to nitric acid (HNO_3) through reaction 1.27.

$$4HNO_2 + 2O_2 \rightarrow 4HNO_3 \quad (1.27)$$

The nitric acid can easily dissociate in wet conditions and release protons, increasing the concentration of protons at the cathode, which in turn causes cell performance degradation [23].

1.7.7 Sulfur Dioxide

Sulfur dioxide (SO_2) exists in air, especially in heavily trafficked areas and agricultural areas [8]. SO_2 can poison the fuel cell both by occupying the Pt surface and by decreasing the pH-value inside the MEA, resulting in free acids in the MEA and causing potential drop [8].

After experiments with 2.5 ppm and 5 ppm SO_2 in air, Mothadi *et al.* [24] saw that the cathode overpotential was higher after exposing the fuel cell to 5 ppm SO_2/air for 23 hours compared to when they exposed it to 2.5 ppm SO_2/air for 46 hours. They concluded that there is a concentration gradient effect for the SO_2 poisoning. They obtained partial recovery after applying clean air for 24

hours. The recovery in clean air after exposing the cell to 2.5 ppm SO_2/air was smaller than the recovery after exposing it to 5 ppm SO_2/air. Cyclic voltammetry was needed to obtain full recovery. The cyclic voltammetry showed one oxidation peak at 0.89 V and one at 1.05 V. The two peaks correspond to two different sulfur species adsorbed on the Pt catalyst surface. The formations of the two sulfur species are represented in reaction 1.28 and 1.29.

$$SO_2 + 2H^+ + 2e^- \rightarrow Pt\text{-}SO + H_2O \quad (1.28)$$

$$Pt\text{-}SO + 2H^+ + 2e^- \rightarrow Pt\text{-}S + H_2O \quad (1.29)$$

1.8 Mitigation Strategies

The first step in contamination mitigation is to remove the contaminant from the hydrogen gas, before it reaches the fuel cell. It is however not always possible or cost efficient to remove all the contaminants from the hydrogen. The second step is therefore to mitigate the poisoning effect on the fuel cell.

1.8.1 Carbon Monoxide Removal

Removal of CO from the hydrogen fuel can be divided into two methods; Deep removal and hydrogen purification. The deep removal of CO involves the following reactions:

$$CO + H_2O \rightarrow CO_2 + H_2 \qquad \Delta H_{298} = -41 \text{ kJ/mol} \quad (1.30)$$

$$CO + \tfrac{1}{2}O_2 \rightarrow CO_2 \qquad \Delta H_{298} = -283 \text{ kJ/mol}, \quad (1.31)$$

$$CO + 3H_2 \rightarrow CH_4 + H_2O \qquad \Delta H_{298} = -205.8 \text{ kJ/mol} \quad (1.32)$$

which are accompanied by the following side reactions:

$$CO_2 + 4H_2 \rightarrow CH_4 + 2H_2O \qquad \Delta H_{298} = -164.6 \text{ kJ/mol} \quad (1.33)$$

$$H_2 + \tfrac{1}{2}O_2 \rightarrow H_2O \qquad \Delta H_{298} = -241.8 \text{ kJ/mol}. \quad (1.34)$$

To accomplish CO deep removal, a two-step process is required. The first step increases the CO local concentration by CO adsorption onto a catalyst surface. This can be achieved because the CO-catalyst bond is stronger than the H-catalyst bond. In the second step, the adsorbed CO is converted into CO_2, as in eq 1.30 and 1.31 (preferential oxidation) or CH_4, as in eq 1.32 (methanation). The CO methanation is operated at temperatures from 180 to 280 ˚C and is therefore not suitable for mobile applications. The CO preferential oxidation is more suitable since it only requires a temperature of 80 ˚C to 180 ˚C. [8]

Adsorption of Species other than Hydrogen

Two types of adsorption-based hydrogen purification technologies are temperature swing adsorption (TSA) and pressure swing adsorption (PSA). With these technologies, the temperature/pressure is varied. The contaminant is adsorbed during low temperature/high pressure and desorbed under high temperature/low pressure. The TSA is a slower process than PSA and is therefore only applicable when the contaminant concentration is quite low. The PSA process can provide hydrogen with a purity of up to 99.999 %. [8]

Cryogenic Separation

The contaminants have different boiling point than hydrogen, which can be used for cryogenic separation. Under a pressure of 12 atm, the temperature needed to separate hydrogen from a liquid mixture of CO and CH_4 is -237 ˚C. The low working temperature makes the process very costly. [8]

1.8.2 Carbon Monoxide Poisoning Mitigation

The methods for CO poisoning mitigation can generally be divided into two groups; removal of adsorbed CO by oxidation to CO_2, and minimization of CO adsorption. In the following, three ways of mitigating CO poisoning are described; oxidant bleeding, developing CO tolerant catalysts and optimizing operating conditions.

Oxidant Bleeding

Oxidant bleeding means that oxygen is mixed into the fuel stream before the fuel inlet to the fuel cell. This reduces the CO levels by the water gas shift reaction (eq 1.30) mechanism and selective oxidation of CO (eq 1.31). Instead of oxygen, air or hydrogen peroxide (H_2O_2) can be used with the same effect. Experiments have shown that an addition of 2 % to 5 % O_2 to a fuel stream with CO levels up to 500 ppm, can restore the performance of the fuel cell to a CO-free cell performance. Advantages with oxygen/air bleeding are simplicity, effectiveness, and economic value. One disadvantage with oxygen/air bleeding is that only 0.25 % of the O_2 molecules oxidize an adsorbed CO molecule. The other O_2 molecules chemically combust with H_2 and therefore lower the fuel cell efficiency and may also accelerate sintering of the catalyst. One advantage of using H_2O_2 instead of oxygen/air is that H_2O_2 can be stored as a liquid and be added to the humidification water, preventing safety issues when handling H_2O_2 gas mixtures in the presence of the catalyst. However, disadvantages with H_2O_2 bleeding, as well as oxygen/air bleeding, are degradation and stability issues. [8]

One way to reduce the amount of air at the anode and still keep the CO removal effect may be to use pulsed air bleed (PAB). With PAB, the air bleed is shut off periodically. This technique may be effective because the voltage recovery in the presence of air bleed is faster than the voltage drop during CO poisoning in the absence of air bleed. [25]

Carbon monoxide Tolerant Catalysts

The catalyst type affects the severity of the poisoning phenomena because it determines the kinetics of CO adsorption and oxidation [8]. CO tolerant catalysts consist of Pt, alloyed or co-deposited with one or more other metals. The platina/ruthenium (PtRu) catalyst is to date the best CO tolerant catalyst. Other Pt-based alloys that have shown to have high tolerance to CO poisoning are:

- Binary (PtM, with M=Mo, Nb, Ta, Sn, Co, Ni, Fe, Cr, Ti, Mn, V, Zr, Pd, Os, Rh)
- Ternary (PtRuM, with M=Mo, Nb, Ta, Sn, Co, Ni, Fe, Cr, Ti, Mn, V, Zr, Pd, Os, Rh)
- Quaternary (PtRuMoNb)
- Pt-based composite-supported (PtRu-H_xMO_3/C, (with M=W, Mo) and organic and metal complexes.)

The effects that can make a Pt alloy more CO-tolerant than pure Pt are the bifunctional effect, the electronic effect, and the ensemble effect. With the bifunctional mechanism, the water first reacts with the alloying metal (M, *e.g.* Ru) and forms M-OH_{ads}, which then oxides the CO adsorbed onto the Pt. This is described in the following reactions:

$$M + H_2O \rightarrow M_e\text{-}OH_{ads} + H^+ + e^- \quad (1.35)$$

$$Pt\text{-}CO_{ads} + M\text{-}OH_{ads} \rightarrow Pt + M + CO_2 + H^+ + e^- \quad (1.36)$$

With the electronic effect, M alters the electronic properties of the catalytically active Pt, which reduces the strength of the Pt-CO bond. The ensemble effect means that M alters the distribution of the Pt, which enables different reaction pathways for hydrogen adsorption and oxidation.

It is not only the composition of the catalyst that affects its CO tolerance, but also the preparation methods. With the right preparation methods, a better control of particle-size distribution and the chemical composition of catalysts can be obtained. Preparation methods that have shown good results are high energy ball-milling, synthesis using $Na_2S_2O_3$, and combustion synthesis. It has also been shown that a composite anode structure may improve the CO tolerance. [13]

Optimizing Operating Conditions

The flow rate, temperature, relative humidity, and pressure are operating conditions that affect the CO poisoning. The CO poisoning effect is increased with an increased flow rate. An increase in temperature mitigates the CO poisoning because the CO adsorption is decreased. With a higher relative humidity, the CO adsorption is decreased because of higher H_2O and OH coverage. Another way to decrease the CO adsorption is to lower the partial pressure of CO by lowering the anode pressure. [8]

1.8.3 Carbon Dioxide Removal

CO_2 removal can be divided into two types; CO_2 separation based on a low temperature liquid absorbent solution and CO_2 separation based on solid sorbents at high temperatures. The most common process is CO_2 absorption by amines. Typically, CO_2 is absorbed by amines at a temperature of 25 ˚C to 80 ˚C and using a pressure of around 70 atm. A novel CO_2 separation technique based on solid sorbents at high temperatures is called Sorption-Enhanced Hydrogen Production (SEHP). The technique produces H_2 in one step, combining hydrocarbon reforming, water gas shift, and CO_2 separation reactions. When using methane, the SEHP process can be expressed as:

$$CH_{4(gas)} + 2H_2O_{(gas)} + Sorbent_{(solid)} \rightarrow 4H_{2(gas)} + Sorbent\text{-}CO_{2(solid)} \quad (1.37)$$

With SEHP, the hydrogen produced is purer than hydrogen produced with conventional steam reforming of methane. This reduces the necessity of hydrogen purification. [8]

1.8.4 Carbon Dioxide Poisoning Mitigation

Because CO production is the main poisoning mechanism of CO_2, mitigation methods of CO_2 contamination are similar to those of CO contamination. The CO tolerant catalysts PtRu and PtMo have been compared in the case of CO_2 contamination and the PtRu catalyst showed better results. Several experiments have shown that oxygen bleeding mitigates the CO_2 poisoning effect. [14]

1.8.5 Hydrogen Sulfide Removal

There are three ways of removing H_2S from the fuel feed; chemical absorption, partial oxidation and decomposition. In the chemical absorption method, the H_2S reacts with a metal oxide or a metal hydroxide and forms water and metal sulfide, as in the following reactions

$$H_2S_{(g)} + ZnO_{(s)} \rightarrow H_2O + ZnS_{(s)} \quad (1.38)$$

$H_2S_{(g)} + 2NaOH_{(aq)} \rightarrow 2H_2O + Na_2S_{(aq)}$. (1.39)

The advantages with this method are that a fast reaction rate can be achieved under ambient conditions and the H_2S can be removed completely. The disadvantage is that the metal sulfide needs a post-treatment. In the partial oxidation method, H_2S is converted into S and H_2O in an exothermic process. One commercialized technology using the partial oxidation method is the Clause plant [8]. In a Clause plant, the following reactions take place

$2H_2S + 3O_2 \rightarrow 2SO_2 + 2H_2O$ (1.40)

$2H_2S + SO_2 \rightarrow 3S + 2H_2O$. (1.41)

SO_2 is formed from H_2S in the first reaction and reacts with the remaining H_2S in the second reaction to form elemental sulfur. Disadvantages with this method are that the hydrogen is "lost" in the water that is formed and a tail gas with mainly SO_2 is generated, which requires a treatment to minimize environmental impact. The decomposition of H_2S is expressed in the following reaction

$H_2S(g) \rightarrow H_2(g) + S$. (1.42)

One advantage with this method is that both sulfur and hydrogen are recovered as products. The disadvantage is that the reaction is highly endothermic and therefore needs additional thermal energy. Temperatures higher than 1500 ˚C and a rapid cooling system are needed for direct decomposition. Via thermochemical cycles, the overall decomposition reaction can be obtained at lower temperatures. [8]

1.8.6 Hydrogen Sulfide Poisoning Mitigation

H_2S adsorbs even more strongly than CO to the Pt catalyst and the poisoning effect is therefore much stronger. As in the case of CO contamination, the H_2S adsorption is decreased with an increase in temperature and decrease in H_2S concentration and fuel flow. As opposed to CO poisoning, using a Pt alloy instead of pure Pt as the catalyst do not result in sufficient tolerance to H_2S poisoning [13] and a H_2S poisoned cell is only partly recovered when neat H_2 is introduced to the cell. It has been shown that cycling the current is the most effective measure to recover the fuel cell performance from H_2S poisoning. H_2S adsorbs dissociativly onto the anode, which leads to adsorbed sulfur. To oxidize the adsorbed sulfur, potentials higher than the dissociation potentials are needed. The dissociation potentials are 0.4 V at 90 ˚C, 0.5 V at 60 ˚C, and 0.6 V at 30 ˚C. It has been shown that 95 % recovery from H_2S poisoning can be achieved after a cyclic voltammetry treatment with potentials higher than the dissociation potential. [8]

Lopes *et al.* [26] showed that air bleed might slightly mitigate the poisoning effect of H_2S by oxidizing some of the sulfur adsorbed onto the catalyst surface to SO_2.

1.8.7 Ammonia Removal

Since the poisoning effect of ammonia is severe even at a level of 1 ppm NH_3, the removal of ammonia from the fuel stream is of great importance for the fuel cell performance. Ammonia can be removed from the fuel stream by adsorption in an acid trap. [16]

1.8.8 Ammonia Poisoning Mitigation

There may be ways to mitigate the ammonia poisoning on the anode on a PEM fuel cell through design and choice of materials for the PEM fuel cell. To change the catalyst material may be one

option. The change of catalyst may mitigate the poisoning in two ways; enhancement of the oxidation rate of ammonia on the anode or making the hydrogen oxidation reaction less affected by the presence of ammonia on the anode. When Halseid *et al.* [16] compared the effects of ammonia on an MEA with Pt anode catalyst and an MEA with PtRu anode catalyst they found that the effect was very similar. Changing the catalyst at the cathode side may have a stronger effect on the ammonia poisoning [16].

1.8.9 Nitrogen Oxides Poisoning Mitigation

The NO_x poisoning of the cell can be recovered by applying clean air for several hours and by CV scanning. With these methods the fuel cell performance can be almost fully recovered after NO_x poisoning [8].

1.8.10 Activated Carbon for Contaminant Removal

Activated carbon can be used for removal of organic substances. The organic vapors can be absorbed by an activated carbon block. The absorption capacities for different organic compounds are affected by temperature, pressure, and gas composition. The carbon block needs to be replaced after a certain breakthrough time, when a certain amount of a contaminant breaks through the carbon block. A lower temperature increases the service lifetime of the carbon block, provided that the relative humidity is not increased. With an increase in relative humidity, more water vapor will be adsorbed onto the carbon, hindering the adsorption of the organic vapors. The adsorption capacities for low molecular hydrocarbons, such as ethane and propane have been shown to be low. [27]

Ma *et al.* [28] examined the effectiveness of purifying air from NO_x and SO_2 with activated carbon modified by potassium hydroxide (KOH). They tested samples of activated carbon with different KOH loadings (0 wt.%, 2.2 wt.%, 5.3 wt.%, 10.1 wt.% and 18.3 wt.%) and found that a KOH loading of 10.1 wt.% gave best result. They therefore continued the experiments with activated carbon with that loading. When they exposed a 250 W PEMFC stack to air with 1100 ppb NO_x ($NO:NO_2$=9:1) and 250 ppb SO_2, the stack performance decreased with 30.7 %. When the AC loaded with KOH was used as protection there was no difference in stack performance for the first 130 hours compared to when clean air was used. After further exposure time, the fuel cell stack performance decreased with 1.6 %. When experiments were performed with co-existence of CO_2 they found that the adsorption capacity of NO_x and SO_2 was not affected. They therefore concluded that AC loaded with KOH is a potential filter material for protecting PEMFC from the poisoning by NO_x and SO_2.

Chapter 2

Methods

The experiments in this thesis were performed in laboratories in three different places; PowerCell, Volvo GTT/ATR and KTH.

2.1 Experiments performed at PowerCell Sweden AB

2.1.1 The Fuel Cell Stack

The experiments at PowerCell were performed on a PowerCell S1 fuel cell stack consisting of two cells with Gore MEAs with an active area of 205 cm^2 each.

2.1.2 Experimental Setup

Figure 2.1 shows the experimental setup. Coolant water was supplied to the stack to maintain the desired stack temperature. Humidified air was supplied to the cathodes. Humidified hydrogen and nitrogen gas was supplied to the anodes. When CO was used as contamination it was supplied to the anodes through the humidifier as well. The CO_2 gas was supplied dry to the anode.

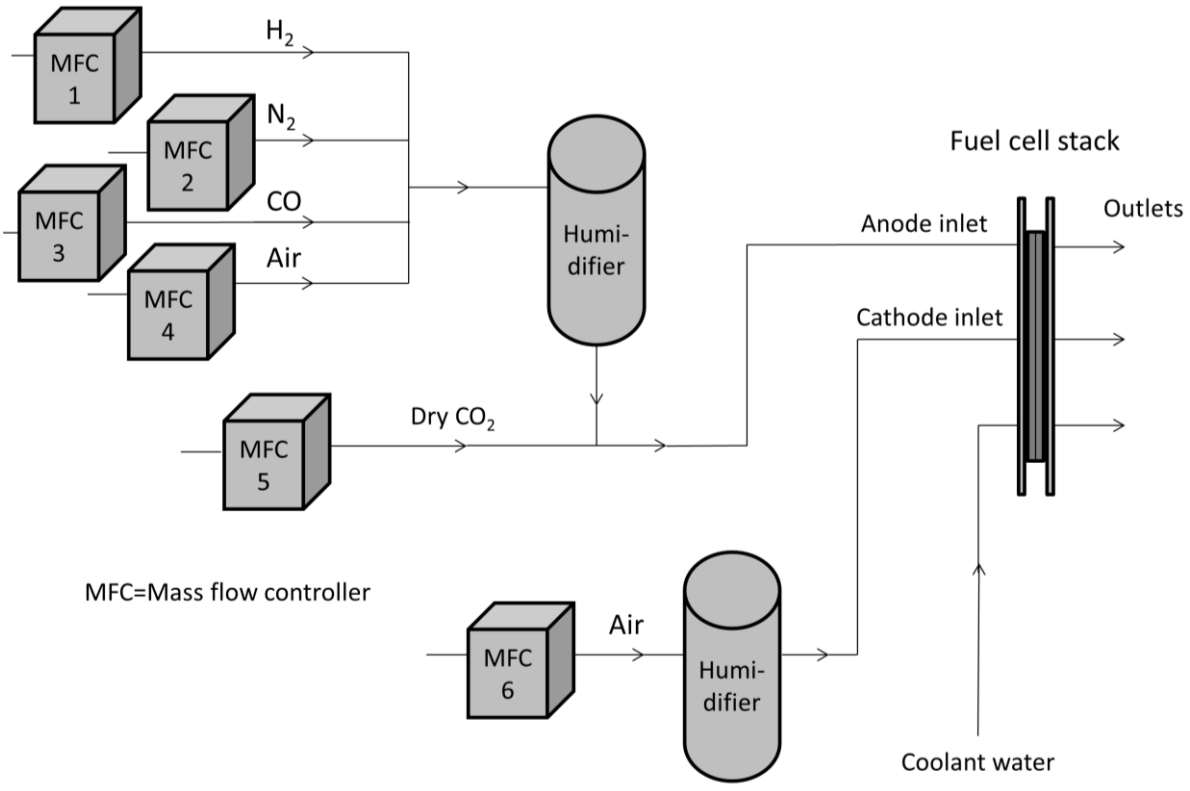

Figure 2.1: Fuel cell stack experimental setup at PowerCell Sweden AB.

2.1.3 Electrochemical Activation

When tests were made on fuel cells at PowerCell, a certain gas mix consisting of H_2, N_2 and CO_2 was used as fuel to simulate a reformate. Air was supplied on the cathode side of the cell. The contaminants were added to the fuel in ppm levels. The temperatures used during all measurements were the following:

Anode inlet: 80 ˚C Anode humidifier: 75 ˚C

Cathode inlet: 80 ˚C Cathode humidifier: 75 ˚C

Coolant (cell): 80 ˚C

The temperatures were held like this to avoid condensation in the pipes or inside the fuel cell. Before any measurements were made to the fuel cell stack, the stack was activated using the following procedure:

Anode stoichiometry: 2 Cathode stoichiometry: 2.5 Stack coolant flow: 2 l/min water

The anode stoichiometry determines the hydrogen flow as a function of how much hydrogen needed for a certain current. If the anode stoichiometry is set to 1, the hydrogen supplied is exactly the same amount as needed to have the set current. A low anode stoichiometry leads to a low amount of waste hydrogen but it also increases the risk of hydrogen shortage. The cathode stoichiometry determines the air supply as a function of how much air needed for a certain current.

The current was first set to 20.5 A for 5 minutes, then 143.5 A for 5 minutes and finally 205 A for 5 minutes. It was then cycled like this for 4 hours. In the final cycles of this activation process no improvement of the stack performance could be seen, indicating that the activation process was completed. The cell voltage during the activation process is plotted in fig 2.2.

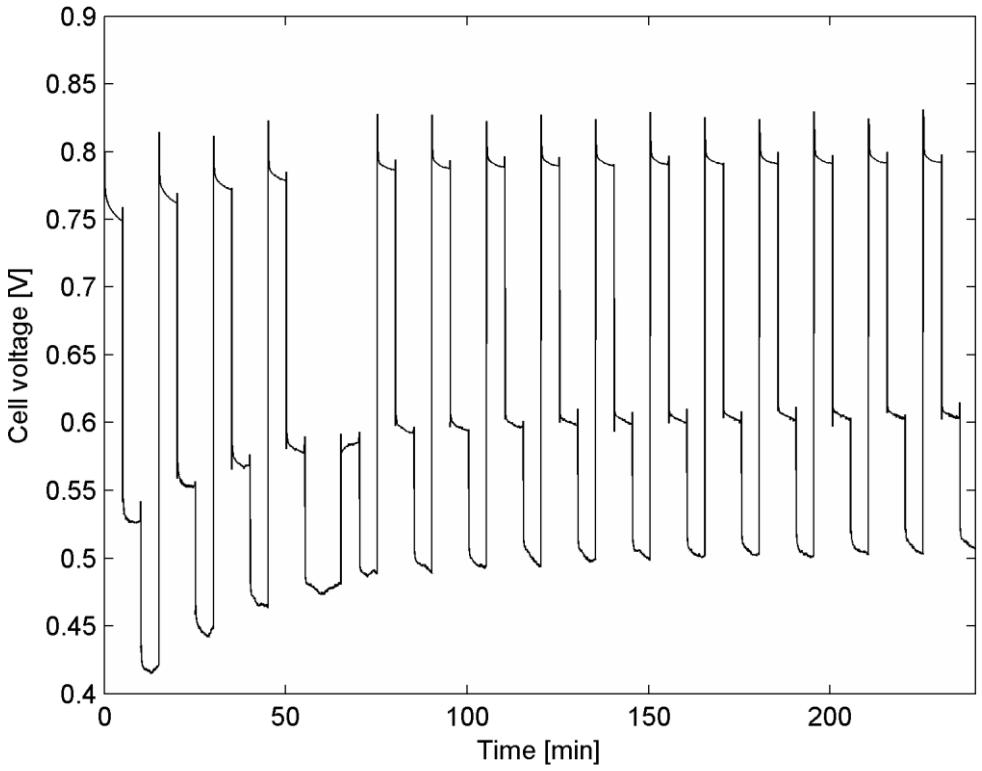

Figure 2.2: Cell voltage during the activation process.

After the stack had been activated, the poisoning tests could be performed.

2.1.4 Carbon Monoxide Contamination

The following settings were used during all CO contamination measurements:

Anode stoichiometry: 2 Cathode stoichiometry: 2.5 Coolant flow: 2 l/min

Anode pressure: 0.15 barg Cathode pressure: 0.25 barg Coolant pressure: 0.5 barg

The cell was exposed to CO with the concentrations 10 ppm, 25 ppm and 50 ppm. Before and after the exposure to CO, the cell was run without CO for one hour. The exposure time to CO was one hour. Each measurement thus ran for three hours. The measurements were made both with and without air bleed (AB). When the measurements were made without AB an extra 20 minutes was added with air bleed in the end of the test to ensure full recovery after the poisoning. The dry gas mixture, which simulated a reformate, can be seen in table 2.1. The current density was held constant at 0.5 A/cm^2 during the measurements.

Table 2.1: Dry concentrations of gases in reformate simulating gas mixtures.

	Without air bleed	With air bleed
H_2 [%]	44	44
N_2 [%]	34	34
CO_2 [%]	22	21.5
Air [%]	0	0.5
CO [ppm]	10/25/50	10/25/50

Measurements were also performed with pulsed AB to examine if better CO mitigation could be achieved with the same total amount of air as when 0.5 % air was supplied continuously. The CO concentration used for these measurements was 50 ppm. Once again, the contamination time was one hour and the cell was run without CO for one hour before and after each contamination. The different air bleed concentrations and pulsing times are represented in table 2.2. The CO_2 concentration was decreased as the air bleed was increased.

Table 2.2: Pulsed air bleed tests.

Air bleed concentration [%]	Air bleed time [s]	Time without air bleed [s]
1	10	10
1	30	30
2	10	30

2.2 Experiments performed at Volvo GTT/ATR

The experimental setup used at Volvo was very similar to the one at PowerCell. The differences were that the stack consisted of one cell instead of two and the contaminants were added in N_2 gas. The gas supplied to the anode was pure, humidified H_2 (with the addition of dry N_2 during contamination) and the gas supplied to the cathode was humidified air. The temperatures were held at the same levels and the activation process was the same as during the experiments at PowerCell.

2.2.1 Ethylene Contamination

Ethylene (CH_2-CH_2) was added from a gas tube containing nitrogen with 1000 ppm ethylene. The contamination levels were 0.1 ppm, 1 ppm, 10 ppm and 100 ppm ethylene. A test with one

concentration consisted of a reference test, a poisoning period and a recovery period. The test procedure for 100 ppm ethylene is presented in table 2.3. When 10 ppm ethylene was used, the nitrogen was instead put to 1 % and so on. The hydrogen flow was constant at 1.42 l/min, thus the total flow increased when nitrogen with ethylene was added.

Table 2.3: The test procedure for ethylene contamination.

	Time [min]	H_2 [%]	N_2 with ethylene [%]	Ethylene [ppm]
Reference test	15	100	0	0
Poisoning	15	90	10	100
Recovery	15	100	0	0

During the measurements, the current was held constant at 0.5 A/cm^2 and the voltage was recorded. A long term test with 4 hours exposure time to 10 ppm ethylene was also done. The recovery after the long term test was 70 minutes long and the current density was then switched between 0.5 A/cm^2 and 0.1 A/cm^2.

2.2.2 Ethane Contamination

Ethane (CH_3-CH_3) contamination tests were performed in the same way as the ethylene contamination tests. The gas tube with nitrogen now contained 1000 ppm ethane and the contamination levels tested were once again 0.1 ppm, 1 ppm, 10 ppm and 100 ppm. The long term test performed with 10 ppm ethylene was performed with 10 ppm ethane as well. The tests were performed on the same fuel cell as the ethylene tests, without changing the MEA.

2.2.3 Hydrogen Sulfide Contamination

The hydrogen sulfide was added to the fuel from a nitrogen tank containing 100 ppm H_2S. At first, tests were performed with 15 minutes contamination of the cell, with the same settings as in the case with ethane and ethylene contamination. The contamination levels were 0.01 ppm, 0.1 ppm, 1 ppm, 5 ppm, 10 ppm and 20 ppm. After contamination with 20 ppm H_2S, a test was made with the same amount of N_2 as when 20 ppm H_2S was added to the H_2, but this time with pure N_2. This test was made to see the impact of the addition of N_2 to the H_2 flow. When all these tests were made, the cell was shut down for three weeks. Then a test was made with pure H_2 to see if time has any impact on the recovery of the fuel cell after H_2S poisoning. All the above tests with H_2S were performed on the same fuel cell as was used to the ethane and ethylene tests.

In addition, a test with longer H_2S exposure time was made, to a fuel cell with a new MEA. The H_2S concentration used in this test was 10 ppm. This concentration was chosen because it was the highest concentration where no effect on the performance was seen during the 15 minutes exposure time experiments. The H_2S exposure time was 4 hours.

2.2.4 Sulfur Dioxide Contamination

The sulfur dioxide was added to the fuel from a nitrogen tank containing 500 ppm SO_2. Before any tests were performed with SO_2, the MEA was changed and activated. The tests were once again performed with 15 minutes exposure time to the contaminant. The SO_2 contamination levels were 0.05 ppm, 0.1 ppm, 1 ppm, 5 ppm, 10 ppm, 20 ppm, 30 ppm and 40 ppm. It was not possible to perform the test with lower contamination levels because of the limited accuracy of the MFCs

available at low flows. The test procedure for the contamination levels 0.05 ppm to 1 ppm was as follows:

- 15 minutes of pure H_2 on the anode
- 15 minutes with the addition of N_2 with SO_2 to the anode gas
- 15 minutes of pure H_2 on the anode
- 3 minutes flushing with pure N_2 on the anode

The test procedure for the contamination levels 5 ppm to 40 ppm was as follows:

- 15 minutes of pure H_2 on the anode
- 15 minutes with the addition of N_2 to the anode gas (same amount as during contamination)
- 15 minutes with the addition of N_2 with SO_2 to the anode gas
- 15 minutes of pure H_2 on the anode
- 3 minutes flushing with pure N_2 on the anode

The reason why pure N_2 was added to the fuel gas during one period was to distinguish the effect of the addition of N_2 to the gas from the effect of SO_2 contamination. This period was not added to the tests with lower SO_2 concentration because the small amount of N_2 added then was assumed to have no effect on the performance.

A long term test was also performed with SO_2, with 4 hours exposure time. Before the experiment, the MEA was changed and the fuel cell was activated. The test was started with pure H_2 on the anode and the constant current 0.5 A/cm^2. It was run like this for 10 minutes to have a reference. The cell was then exposed to 10 ppm SO_2 for 4 hours. When the SO_2 supply was turned off after 4 hours, the recovery process started. After 10 minutes recovery, the current was changed to 0.1 A/cm^2. The current was then shifted between 0.5 A/cm^2 and 0.1 A/cm^2 every 10 minutes for 70 minutes.

2.3 Experiments Performed at KTH

2.3.1 The Test Cell

The experiments performed at KTH were made on test cells with one single Gore MEA each. The active surface area of the MEAs was 3 cm^2. On the anode side the catalyst was Pt/Ru and on the cathode side it was Pt. A Gore Carbel GDL was applied to the anode and cathode side of the MEA. The gas was distributed on the GDL through spiral gas channels.

2.3.2 Experimental Setup

The gas supply to the cell was controlled by mass flow controllers. All gases went through a humidifier before entering the cell, except for some of the hydrogen gas (with or without NH_3), or argon gas (with or without propene), as can be seen in fig 2.3. The humidifiers were filled with milli-Q water, which is purified deionized water. The temperatures were held as follows:

Anode inlet:	85 ˚C	Anode humidifier:	77 ˚C
Cathode inlet:	85 ˚C	Cathode humidifier:	77 ˚C
Cell temperature:	80 ˚C		

Humidifiers: 77 ˚C
Cell: 80 ˚C
Gases supplied to the cell: 85 ˚C

The temperatures were held like this to avoid condensation. The temperatures of the cell and the gases were controlled electrically.

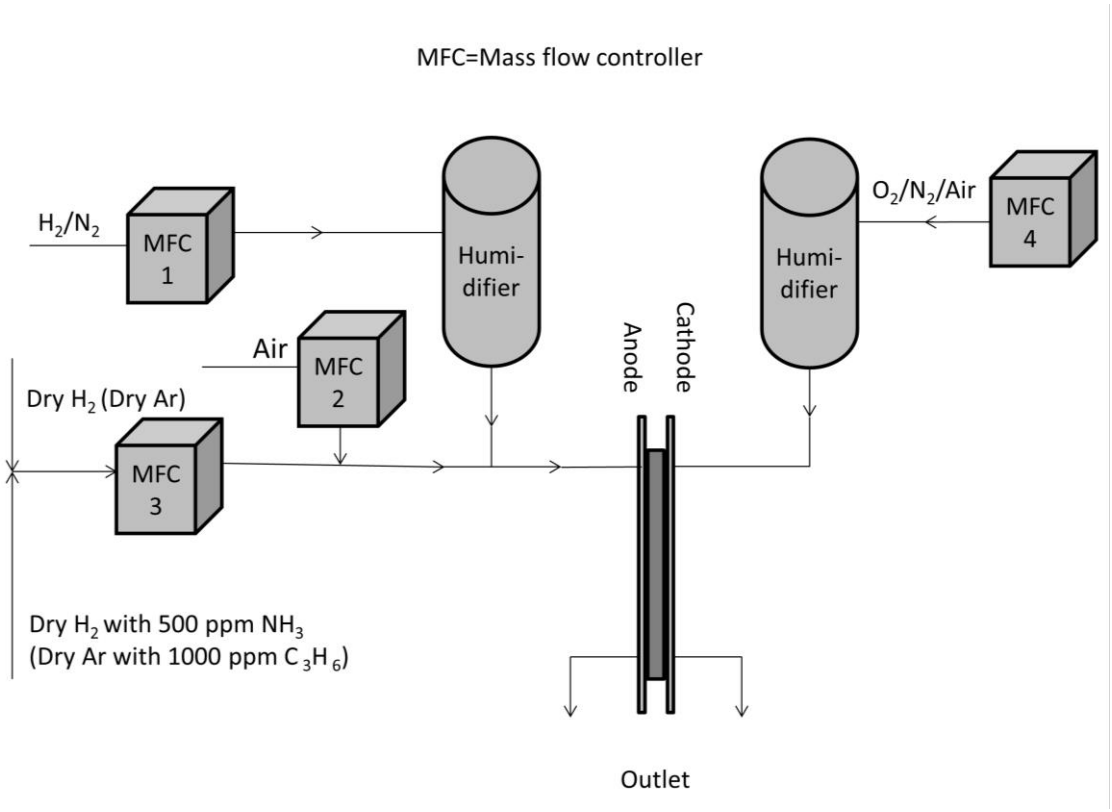

Figure 2.3: Fuel cell experimental setup at KTH.

2.3.3 Electrochemical Activation

The following activation procedure was performed on all test cells before any measurements were made:

1. CV of the cathode: 30 cycles with 100 mV/s scanning rate
2. CV of the cathode: 20 cycles with 50 mv/s scanning rate
3. CV of the cathode: 10 cycles with 100 mV/s scanning rate
4. Current density held constant at 0.5 A/cm^2 for about 15 hours

In point 1-3, the anode gas was 68 ml/min H_2 and the cathode gas was 100 ml/min N_2. In point 4, the cathode gas was changed to 219 ml/min O_2.

2.3.4 Ammonia Contamination

Ammonia was supplied from a gas tube containing hydrogen with 500 ppm NH_3. Two different kinds of ammonia contamination experiments were performed to investigate how ammonia affects the fuel cell. Each experiment was performed with both 200 ppm and 100 ppm ammonia. The contamination time was 3 hours and 20 minutes when the ammonia concentration was 200 ppm and

6 hours and 40 minutes when the ammonia concentration was 100 ppm. The fuel cells in all experiments were thus exposed to the same total amount ammonia.

Experiment type 1: CV and EIS

In this experiment, the effect of ammonia contamination on the cathode was to be examined. This was done with cyclic voltammetry (CV) of the cathode. Thus hydrogen was supplied to the anode and nitrogen to the cathode. The CV was made between 0.1 V and 1.2 V. At first, the hydrogen supplied to the anode was without ammonia. Because pure hydrogen results in more hydrogen crossover than hydrogen diluted with an inert gas, different levels of hydrogen diluted with nitrogen were examined. The subsequent CV tests were made with 40 % hydrogen because this gave a relatively low hydrogen crossover and it was an easy way to get the desired 200 ppm NH_3 during the contamination. The total flow on the anode was decided to be 68 ml/min. The hydrogen flow was thus 27.2 ml/min and the nitrogen flow to the anode was 40.8 ml/min. The nitrogen flow on the cathode was 100 ml/min. The test procedure during the contamination was the following:

1. CV with 4 cycles with scanning rate 100 mV/s
2. CV with 2 cycles with scanning rate 50 mV/s
3. EIS from 1 Hz to10 kHz

This test procedure took approximately seven minutes and it was repeated every ten minutes during the contamination time. The test procedure was also performed once before ammonia exposure, as a reference. After the contamination, a recovery was performed with pure hydrogen on the anode (still diluted with N_2). Two different recovery processes were performed for different MEAs. One was with 600 cycles of CV with scanning rate 100 mV/s. The other recovery process was with one EIS and two cycles of CV with the scanning rate 50 mV/s, repeated every 10 minutes for five hours.

Experiment type 2: Polarization curves and high frequency resistance measurements

During these experiments the anode gas flow was 68 ml/min H_2, whereof 27.2 ml/min and 13.6 ml/min was supplied as dry gas during the experiments with 200 ppm and 100 ppm respectively. The cathode gas flow was 219 ml/min air or O_2. The polarization curves were performed before ammonia exposure, after the cell had been contaminated with ammonia (ammonia was still supplied) and after the recovery. During the contamination and recovery process, high frequency resistance (HFR) measurements were made. The frequency was then swept from 5 kHz to 500 Hz while the impedance magnitude and phase were recorded. One frequency sweep took one minute and a sweep was made every second minute. The current density was held at 0.5 A/cm^2.

2.3.5 Propene

Propene was added from a tube containing 1000 ppm propene in argon. The test procedure was the following:

1. 30 min without propene, current density held at 0.5 A/cm^2
2. 20 hours with 100 ppm propene, current density held at 0.5 A/cm^2
3. Polarization curve with 100 ppm propene

In point 1, the anode gases were 61.2 ml/min H_2 and 6.8 ml/min Ar. In point 2 and 3, the same amount of argon was supplied, but with propene. The test was made both with and without 1 % air bleed. When air was added to the fuel, the hydrogen gas was decreased to maintain the same total flow. The cathode flow was 219 ml/min O_2.

Chapter 3

Results and Discussion

In this chapter, the results from the measurements are presented and discussed.

3.1 Carbon Monoxide

No voltage drop could be observed when 10 ppm CO was added to the fuel, neither with nor without air bleed. When 25 ppm CO was added to the fuel without air bleed, a voltage drop of around 12 mV was observed. The potential started to recover fast when the CO was removed from the fuel. The final millivolt was recovered when air bleed was added after one hour recovery time. It is unclear if the potential would have recovered fully without the addition of air bleed, given more time. There was no observable voltage drop when 25 ppm CO was used with the addition of AB. Figure 3.1 shows the voltage during the tests with 25 ppm CO. In fig 3.1(a) it looks as if the recovery starts before the CO is removed from the fuel. This is just a fluctuation in the voltage.

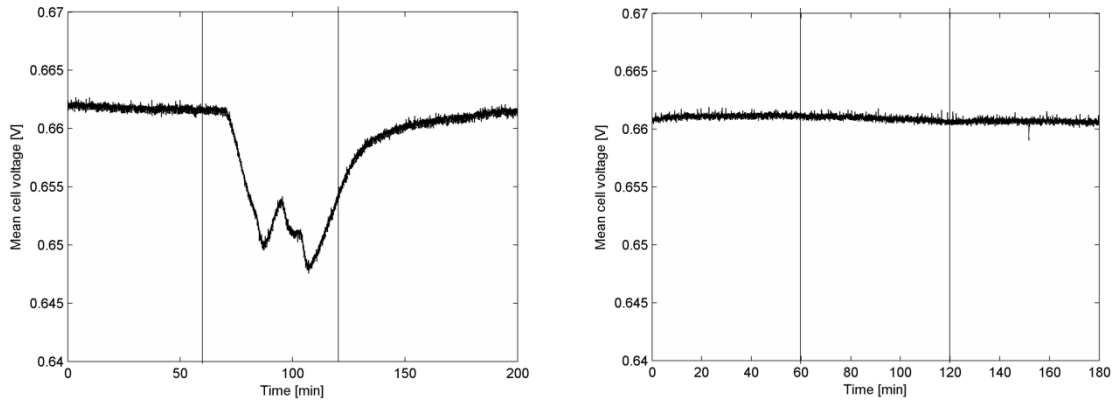

(a) (b)

Figure 3.1: Voltage during constant load. The CO exposure period was from 60 minutes to 120 minutes (between the vertical lines in each graph) and the concentration was 25 ppm. (a) Without AB until 180 minutes. 180-200 min: AB is added to achieve full recovery (b) With AB.

Figure 3.2 shows the voltage during the tests with 50 ppm CO, with and without AB. When 50 ppm CO was added to the fuel without AB, the voltage dropped 17 mV. When the same amount of CO was added during AB, the voltage drop was only 4 mV after one hour exposal and the drop was slower.

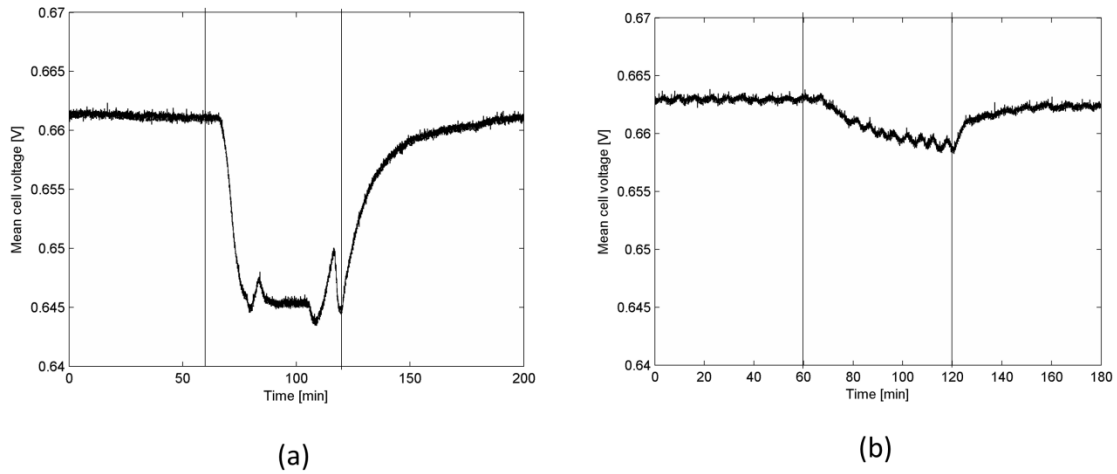

Figure 3.2: Voltage during constant load. The CO exposure period was from 60 minutes to 120 minutes and the concentration was 50 ppm. (a) Without AB until 180 minutes. 180-200 min: AB is added to achieve full recovery (b) With AB.

Figure 3.3 shows the voltage during the tests with different air bleeds. 50 ppm CO is added to the fuel between minute 60 and minute 120. The test sequence started and ended with a constant air bleed of 0.5 %. Note that the start voltage is different for each test, which indicates that the fuel cell did not fully recover between the poisoning periods. The top curve in fig 3.3 (black line) is the voltage during the first test with 0.5 % continuous AB. The bottom curve (blue line) is the final test with 0.5 % continuous AB. The voltages recorded during the tests with differently pulsed air bleeds ended up in between the first and final test with 0.5 % continuous AB.

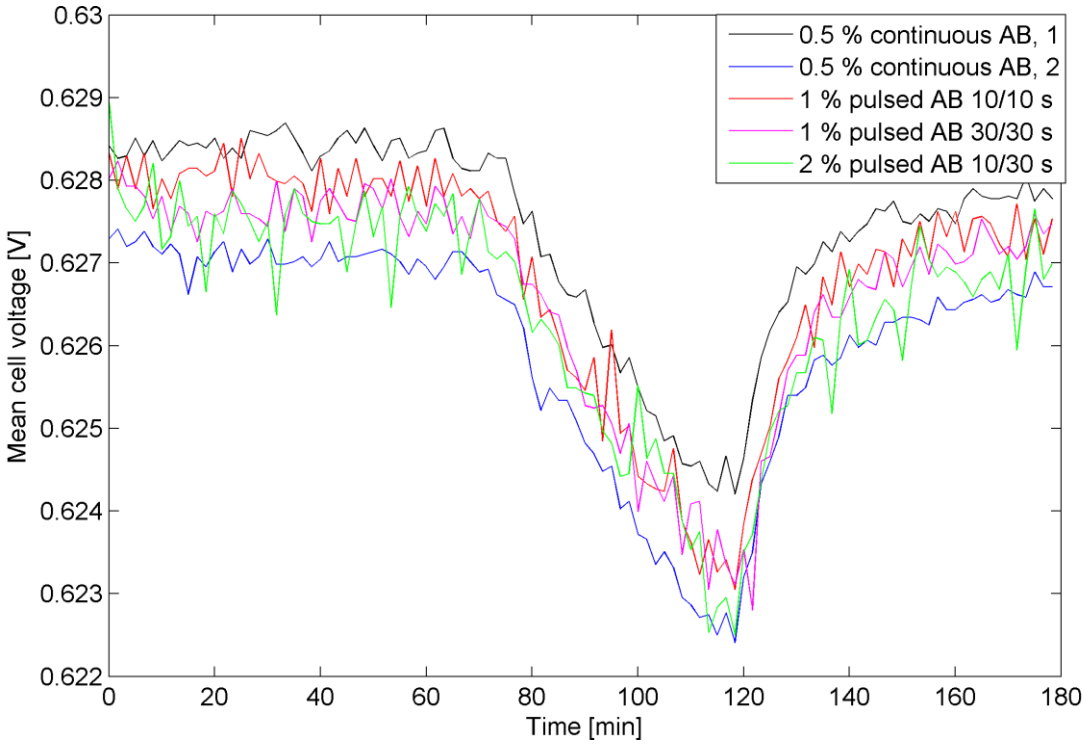

Figure 3.3: Voltage during continuous AB and differently pulsed ABs. All tests performed with 50 ppm CO during the poisoning period. The total amount of air supplied to the fuel is the same for all five tests.

All tests with different ABs showed a voltage drop of 4-5 mV, thus no improvement could be seen when introducing pulsed AB instead of continuous AB. The voltage fluctuated more with pulsed AB than with continuous AB. The reason for the incomplete recovery in these tests could be that similar tests had been made before with the same fuel cell stack. The fuel cell might thus be irreversibly poisoned when exposed to 50 ppm CO during several hours. There is also a risk that the fuel cell is damaged from the addition of air to the fuel containing hydrogen. This risk is greater with higher air bleed however. The experiments made with 0.5 % air bleed and lower CO concentrations did not degrade the fuel cell so it is probably not the air bleed causing the degradation in this experiment either. Experiments made by others have shown that the CO poisoning is completely reversible when air bleed is used. Hui [8] wrote for example that the addition of 5 % O_2 to the fuel stream could fully restore the performance of a fuel cell exposed to 500 ppm CO. It is therefore likely that the performance would have fully recovered in this experiment if higher amounts of air/O_2 had been added to the fuel.

3.2 Ethylene

No performance changes were observed when ethylene was added in concentrations up to 10 ppm. When 100 ppm ethylene was added, some small changes were observed, as can be seen in fig 3.4. The changes were small enough to be considered as insignificant since such small changes could be caused by the addition of 10 % nitrogen. The change in Nernst potential (theoretical OCV) for the fuel cell when the H_2 is diluted to 90 % was calculated (eq 3.1) to see the theoretical effect on the potential from dilution of fuel.

$$\Delta E = \frac{RT}{2F}\left(ln\left(\frac{1}{P_{H_2}90\,\%\sqrt{P_{O_2}}}\right) - ln\left(\frac{1}{P_{H_2}100\,\%\sqrt{P_{O_2}}}\right)\right) =$$

$$\frac{8.3144*353}{2*96485}\left(ln\left(\frac{1}{0.9*\sqrt{0.21}}\right) - ln\left(\frac{1}{1*\sqrt{0.21}}\right)\right) = 1.6\ \text{mV} \qquad (3.1)$$

According to the Nernst equation, the potential should thus decrease with 1.6 mV when the hydrogen is diluted from 100 % to 90 %. Because the fluctuations in the potential are around 50 mV and sometimes greater, a potential drop of 1.6 mV would be difficult to see. A reason for the increased size of the fluctuations when the ethylene was added could be fluctuations in the MFC with which the ethylene was added. These fluctuations could for example affect the water transport in the fuel cell. The result that no voltage drop is observed when 100 ppm ethylene is added to the fuel is consistent with the results from experiments performed by Kortsdottir *et al.* [19]. The experiment with four hours exposure time with 10 ppm ethylene gave no voltage drop either.

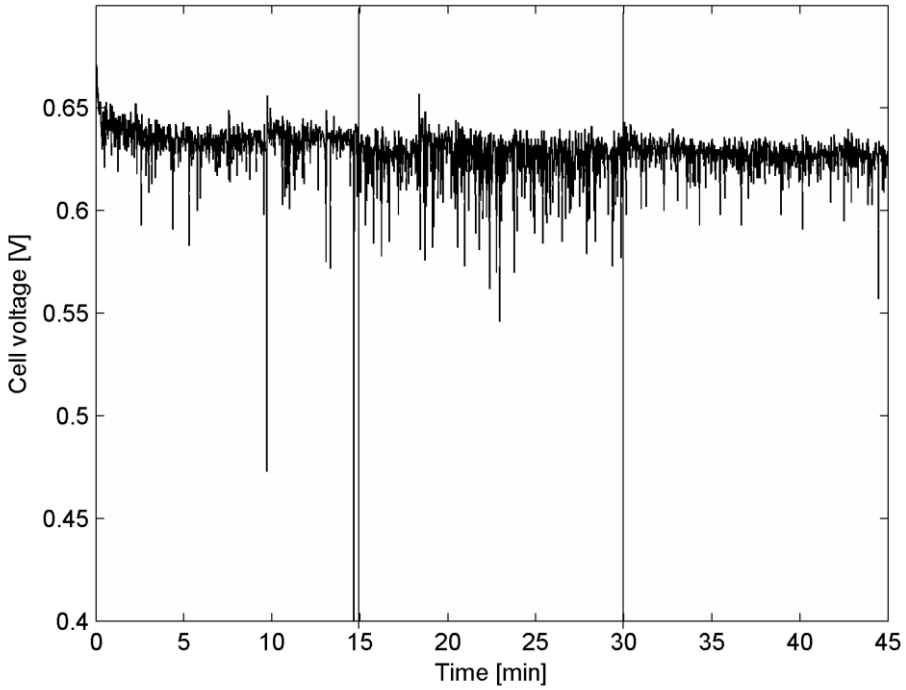

Figure 3.4: Test with 100 ppm ethylene, 0-15 min: Reference, 15-30 min: Poisoning, 30-45 min: Recovery.

3.3 Ethane

Figure 3.5 shows the result from the contamination test with 100 ppm ethane. As in the case with ethylene only small changes can be observed and these changes are probably due to the addition of 10 % N_2. Thus no short-term poisoning effect was observed with 100 ppm ethane. The experiment with four hours exposure time with 10 ppm ethane gave no voltage drop either.

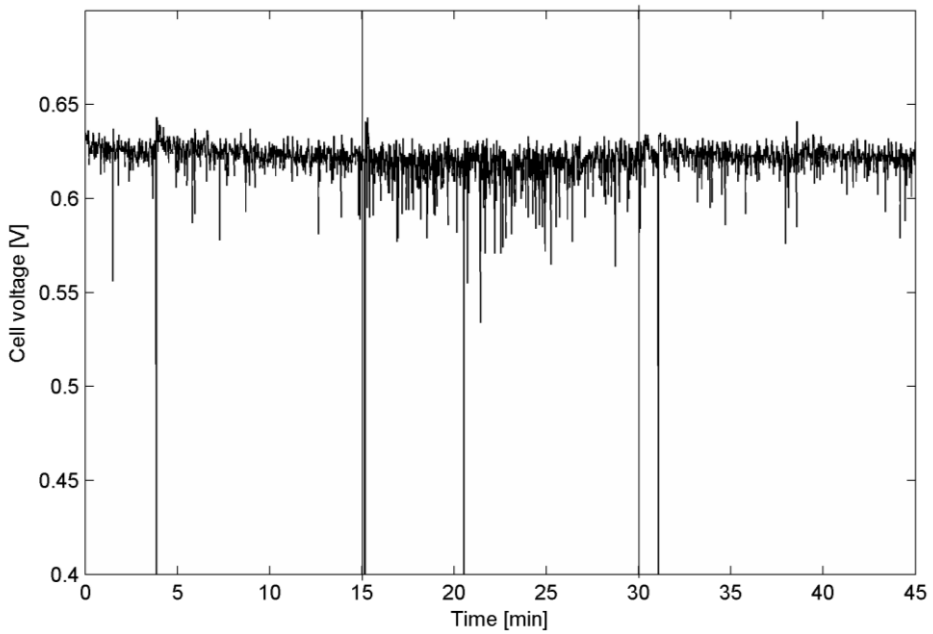

Figure 3.5: Test with 100 ppm ethane, 0-15 min: Reference, 15-30 min: Poisoning, 30-45 min: Recovery.

3.4 Hydrogen sulfide

When the poisoning effect of H_2S was studied, no distinct poisoning effect was seen for H_2S levels up to 10 ppm with the 15 minutes exposure time. Figure 3.6 show the results for the tests with 5 and 10 ppm H_2S. When the fuel cell was exposed to 20 ppm H_2S for 15 minutes, the poisoning effect was clearly visible. The voltage dropped and did not recover during the recovery part of the test. Figure 3.7 shows the result from the test with 20 ppm H_2S (black line) and from a test with pure N_2 (red line). The test with pure N_2 was performed after the test with 20 ppm H_2S. The same amount of N_2 was then added as when 20 ppm H_2S was added to the fuel. From this figure one can conclude that the fluctuations in voltage were due to the addition of N_2 to the fuel stream and that the overall voltage drop was consisting. The overall voltage drop was around 60 mV.

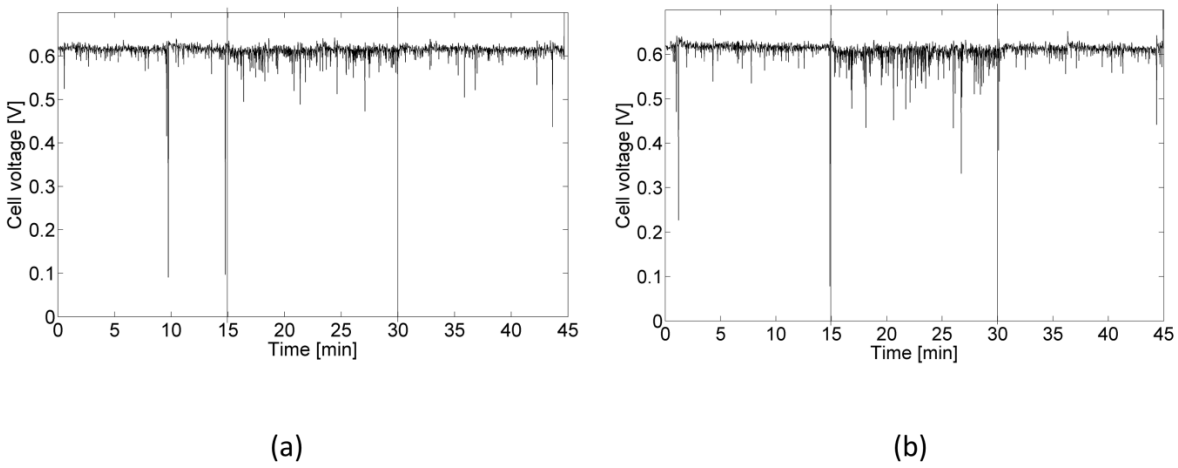

Figure 3.6: (a) Test with 5 ppm H_2S, (b) Test with 10 ppm H_2S. 0-15 min: Reference, 15-30 min: Poisoning, 30-45 min: Recovery.

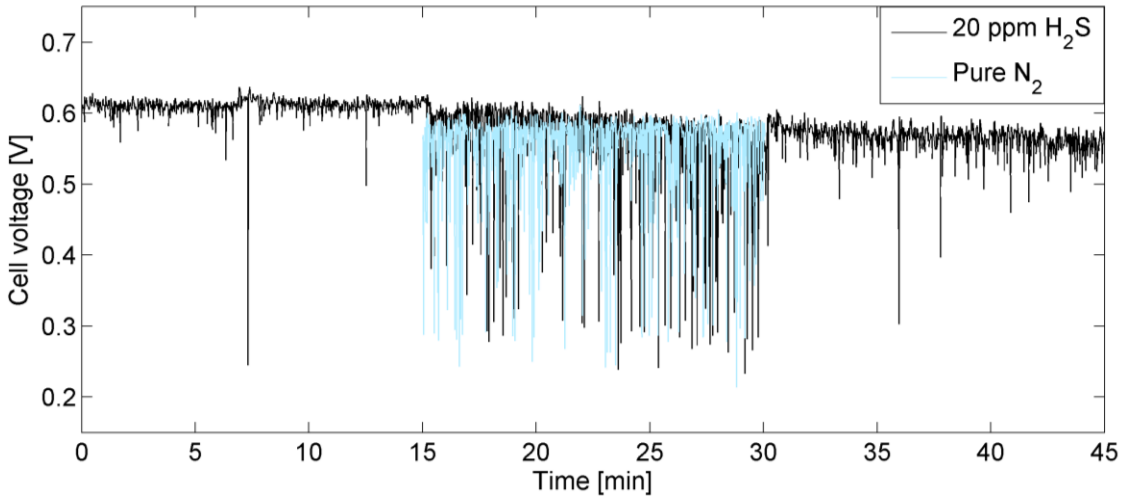

Figure 3.7: Black line: Test with 20 ppm H_2S. 0-15 min: Reference, 15-30 min: Poisoning, 30-45 min: Recovery. Blue line: Pure N_2 applied to the fuel strem for 15 minutes after the test with 20 ppm H_2S.

Figure 3.8 shows the voltage when the fuel cell was run with pure H_2 for 15 minutes before any H_2S contamination, directly after all H_2S contamination tests and three weeks after the poisoning with H_2S. It shows that the fuel cell performance has slightly improved between the test made directly

after the poisoning and the test made three weeks later. This improvement is probably not due to the three weeks, but to the flushing with nitrogen during the shutdown and startup of the fuel cell. There might also have been some H_2S left in the anode gas during the first 15 minutes after the poisoning.

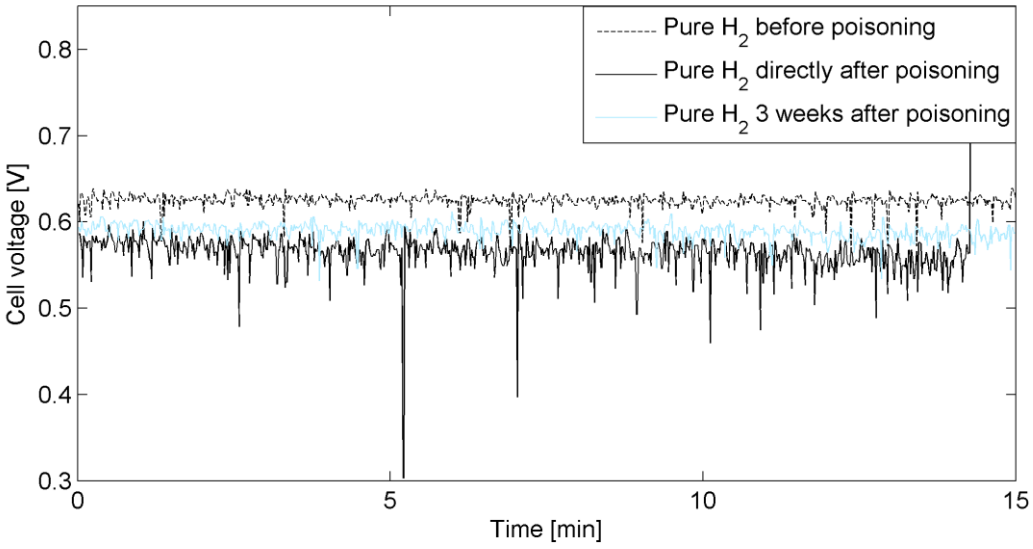

Figure 3.8: Comparison of fuel cell performance before, directly after and 3 weeks after H_2S contamination.

When the fuel cell was exposed to 10 ppm H_2S for four hours, the voltage dropped from 0.64 to 0.32 V, which can be seen in fig 3.9. The voltage drop starts after 30 minutes of contamination and drops then linearly during the following 3.5 hours of contamination. Since the voltage did not reach a steady state during the contamination, it can be assumed that the voltage would have fallen further by an extended exposure time.

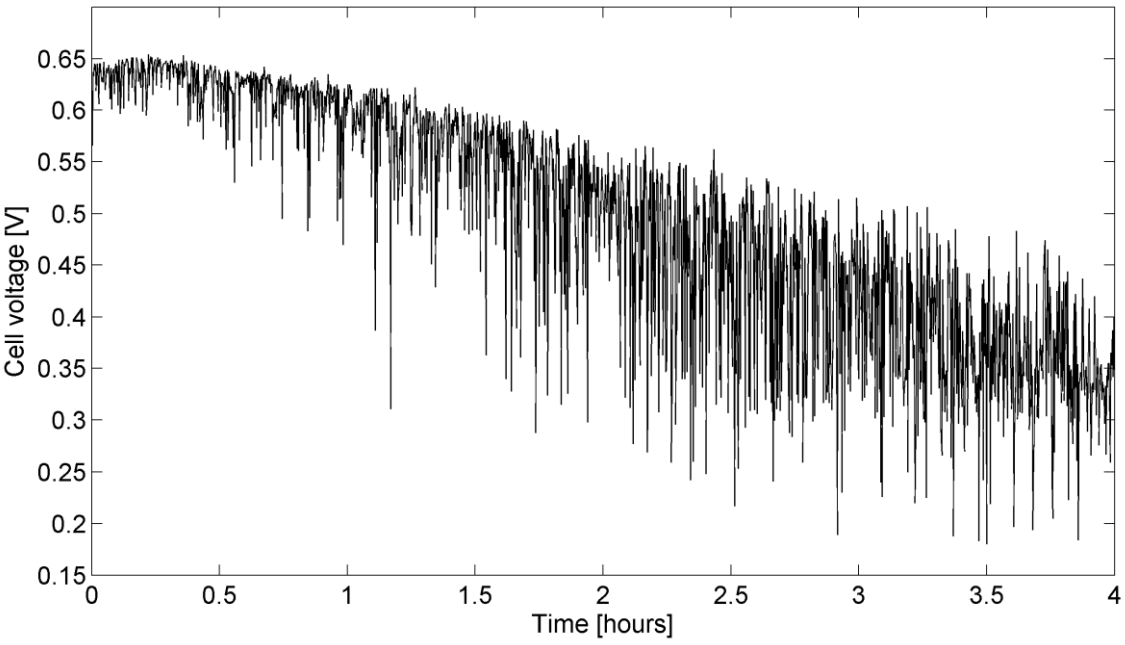

Figure 3.9: Cell voltage during 10 ppm H_2S exposure for four hours.

The result that the H_2S poisoning of the fuel cell depends on the H_2S concentration and exposure time is consistent with results from other experiments, and so is the result that the poisoning is irreversible when just changing the fuel to pure H_2 during recovery [8].

3.5 Sulfur dioxide

When tests were performed with 15 minutes exposure time, no distinct poisoning effect was seen for SO_2 levels up to 20 ppm. Figure 3.10 shows the results for the tests with 5, 10 and 20 ppm SO_2. It is unclear why the test with 10 ppm shows a lower overall voltage but it might be due to a temporarily worse water management in the stack. When the fuel cell was exposed to 30 ppm SO_2 for 15 minutes, the poisoning effect was visible. Figure 3.11 shows the voltage during the tests with 30 and 40 ppm SO_2.

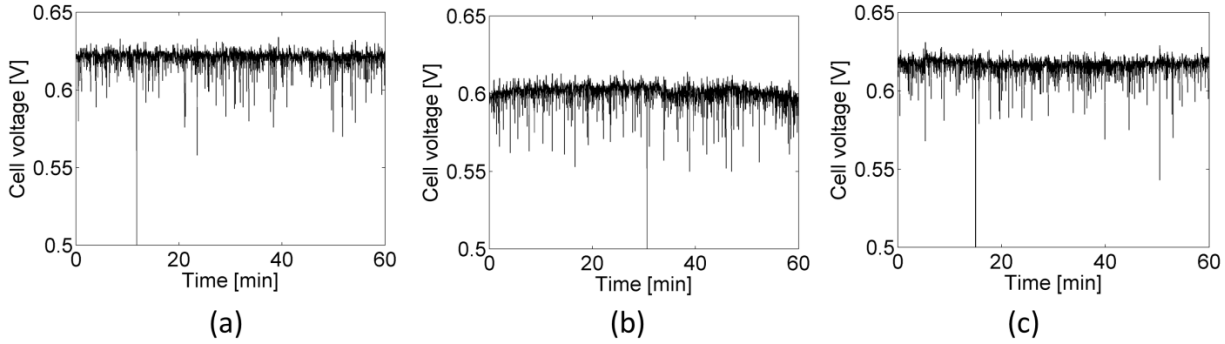

Figure 3.10: (a) Test with 5 ppm SO_2, (b) Test with 10 ppm SO_2, (c) Test with 20 ppm SO_2. 0-15 min: Reference, 15-30 min: addition of pure N_2, 30-45 min: Poisoning, 45-60 min: Recovery.

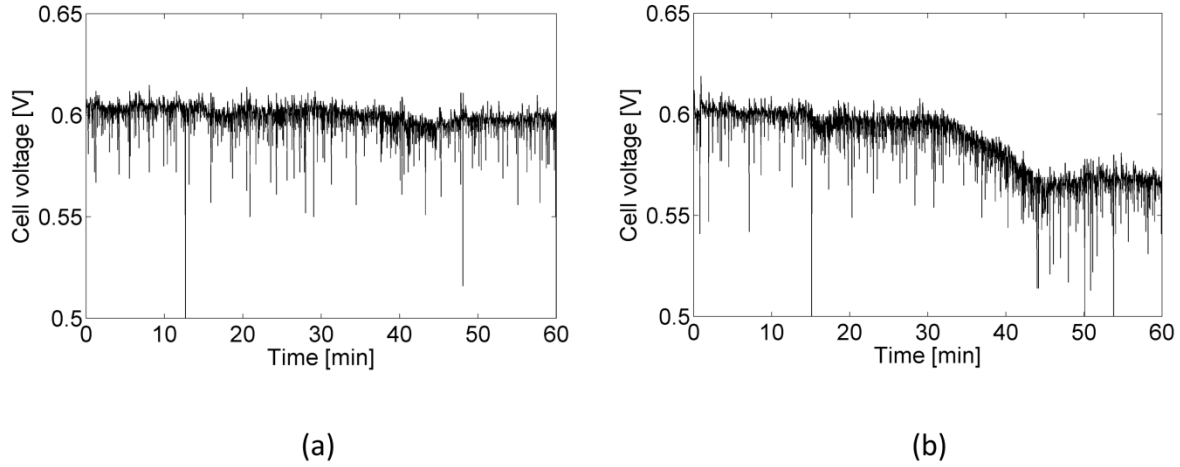

Figure 3.11: (a) Test with 30 ppm SO2, (b) Test with 40 ppm SO2. 0-15 min: Reference, 15-30 min: addition of pure N2, 30-45 min: Poisoning, 45-60 min: Recovery.

Since the MEA was not changed between the tests, there might have been a continuous poisoning of the fuel cell. It is therefore not certain that the poisoning effect will be clearly visible if a fuel cell with a new MEA is exposed to 30 ppm SO_2 for 15 minutes. The tests do however give an approximate concentration for which the fuel cell performance is affected when it is exposed to the contamination for 15 minutes.

When the fuel cell was exposed to 10 ppm SO_2 for four hours, the voltage dropped from 0.62 to 0.56 V, which can be seen in fig 3.12. There was no distinct voltage drop for the first two hours. During the

last two hours of exposure time however, the voltage dropped steadily. The potential drop in the experiment with 10 ppm SO_2 and four hours exposure time was 60 mV and in the experiment with 40 ppm SO_2 and 15 minutes exposure time it was 30 mV. The potential drop was thus twice as big in the long term experiment, but the total amount of SO_2 added was four times as much. This indicates that it is not only the total amount of SO_2 that affects the poisoning of the fuel cell stack, but it is also the instantaneous concentration of SO_2. This concentration gradient was also found by Mothadi *et al.* [24] in their experiments with SO_2 exposure to the cathode.

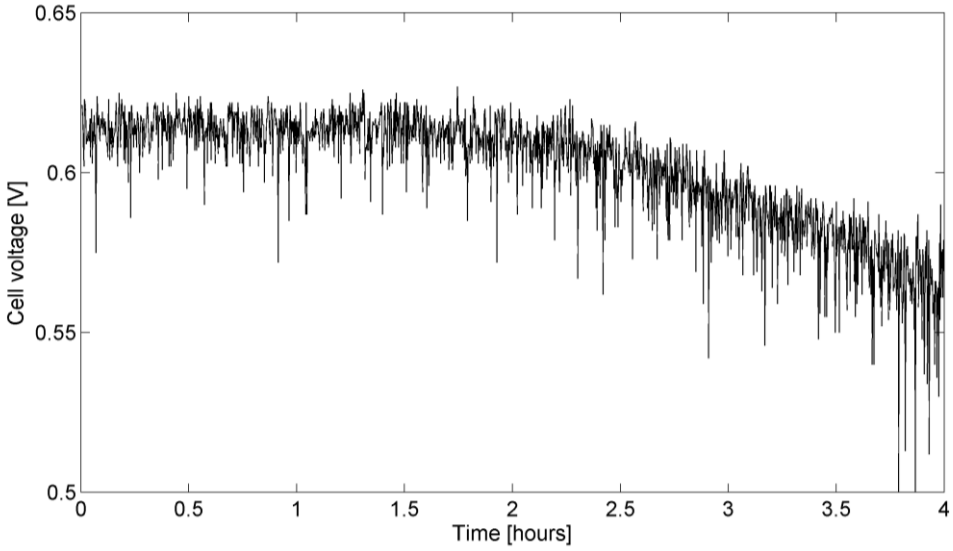

Figure 3.12: Cell voltage during 10 ppm SO_2 exposure for four hours.

Figure 3.13 shows the cell voltage before SO_2 exposure, directly after four hours of SO_2 exposure and after one hour of recovery. The fuel cell performance did not improve during the recovery process, which indicates that the cell is permanently damaged. When the current was changed to 0.1 A/cm^2 during the recovery, the voltage increased to 0.75 V. This increase in voltage was probably not enough to improve the recovery since Mothadi *et al.* [24] found oxidation peaks at 0.89 and 1.05 V during cyclic voltammetry after SO_2 exposure on the cathode.

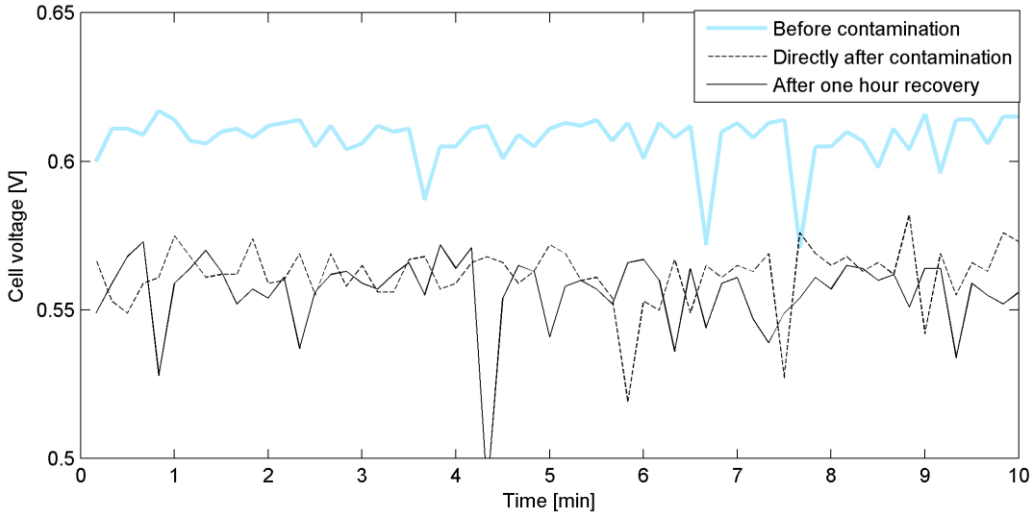

Figure 3.13: Fuel cell voltage before SO_2 contamination, directly after contamination and after one hour recovery.

3.6 Ammonia

3.6.1 Cyclic Voltammetry and Electrochemical Impedance Spectroscopy Measurements

Figure 3.14 shows cyclic voltammetry of the cathode performed with the scan rate 100 mV/s for different concentrations of H_2 diluted in N_2. The double layer region (at approximately 350 mV) should be centered around 0 mA/cm^2 to have minimum hydrogen crossover. This is true for the CV made with 30 % H_2. However, the cyclic voltammetries made with 200 ppm NH_3 were performed with 40 % H_2 since it was convenient when the NH_3 concentration in the gas tube was 500 ppm and it resulted in an acceptable amount of hydrogen crossover.

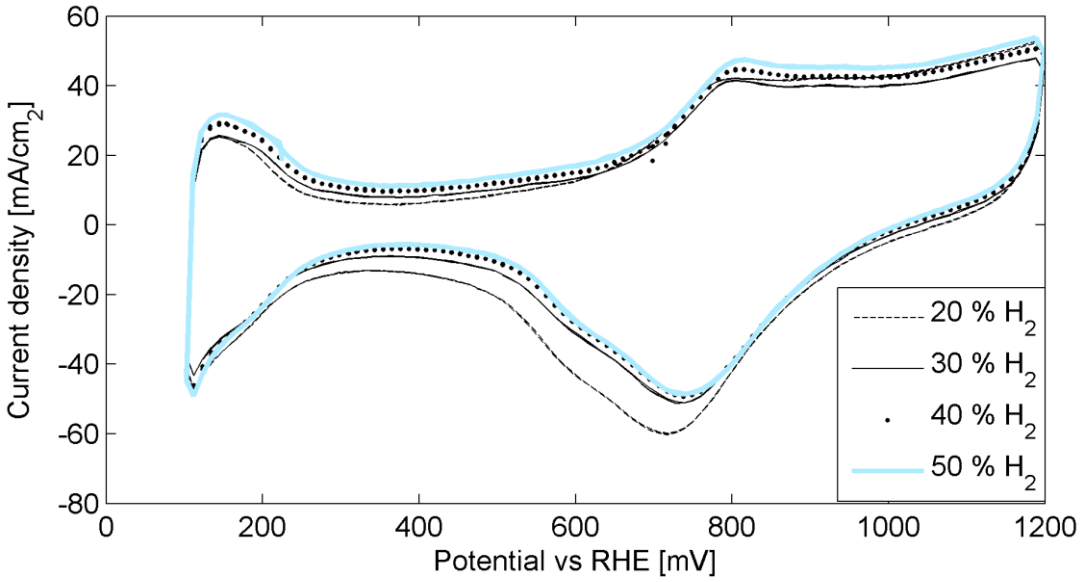

Figure 3.14: Cyclic voltammetry with H_2 diluted in N_2.

Figure 3.15 shows the last cycle from each CV of the cathode with the scanning rate 50 mV/s during contamination with 200 ppm NH_3. The reduction and oxidation peaks decrease as the contamination time increase, until the peaks have totally disappeared. This means that there is virtually no electro active catalyst area left. The CV cycles made from 90 minutes to 200 minutes of contamination are not plotted in fig 3.15 since the difference between those and the CV made after 80 minutes were very small.

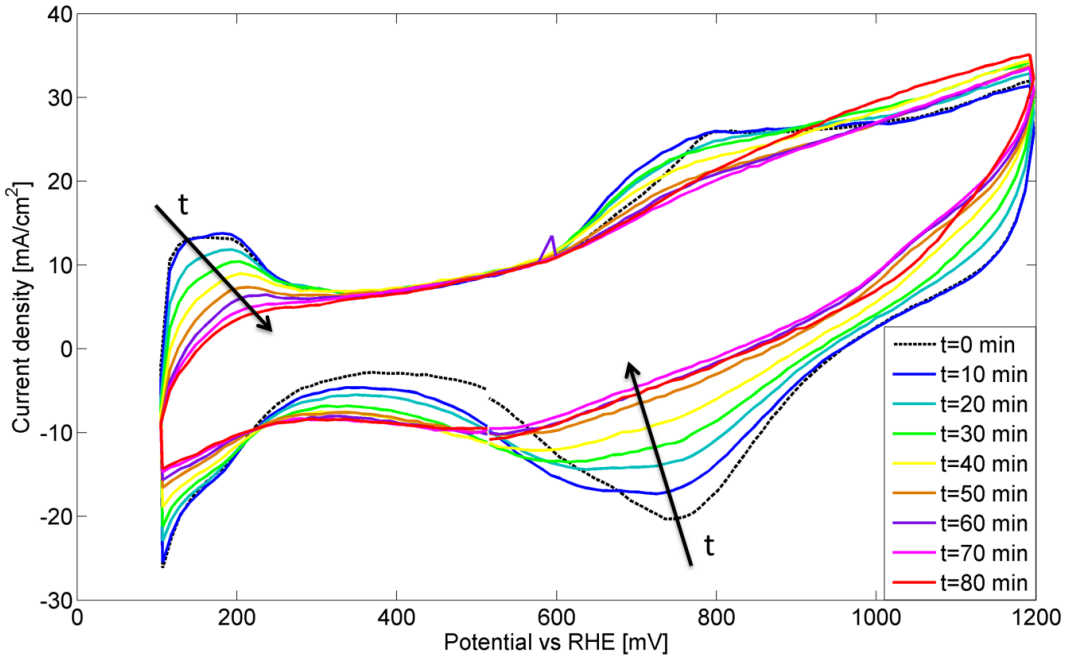

Figure 3.15: Cyclic voltammetry during poisoning with 200 ppm NH3.

The cell did not fully recover after NH_3 exposure during the 600 cycles of CV. Figure 3.16 shows the cycles during recovery with 30 minutes intervals, as well as the CV made before NH_3 exposure. The oxidation and reduction peaks are greater in the CV performed before contamination compared to the last CV in the recovery process. After 180 minutes, the recovery process is very slow. This indicates that the effect of NH_3 contamination on the cathode is probably irreversible. The electro active surface area of the cathode was calculated for the fuel cell before NH_3 contamination and after the recovery by integrating over the peak in the CV around 200 mV, as described in chapter 1.5.4. The electro active catalyst area had decreased with 30 % from the measurement made before NH_3 exposure to the measurement made after the recovery.

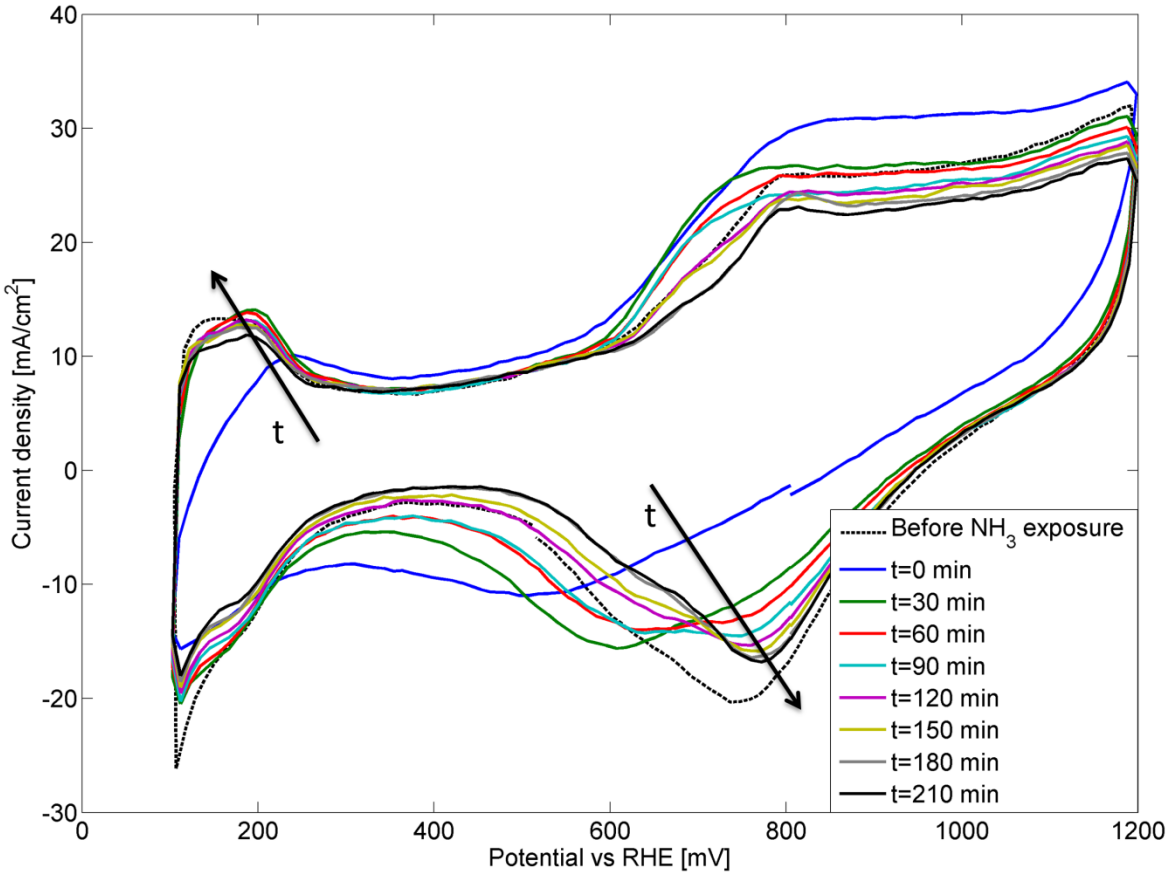

Figure 3.16: CV before NH_3 exposure and during recovery after 200 ppm NH_3 exposure.

Figure 3.17 shows the EIS measurements during contamination with 200 ppm NH_3. It shows that the impedance increases continuously with time during contamination and did not reach a steady state during the 160 minutes contamination time.

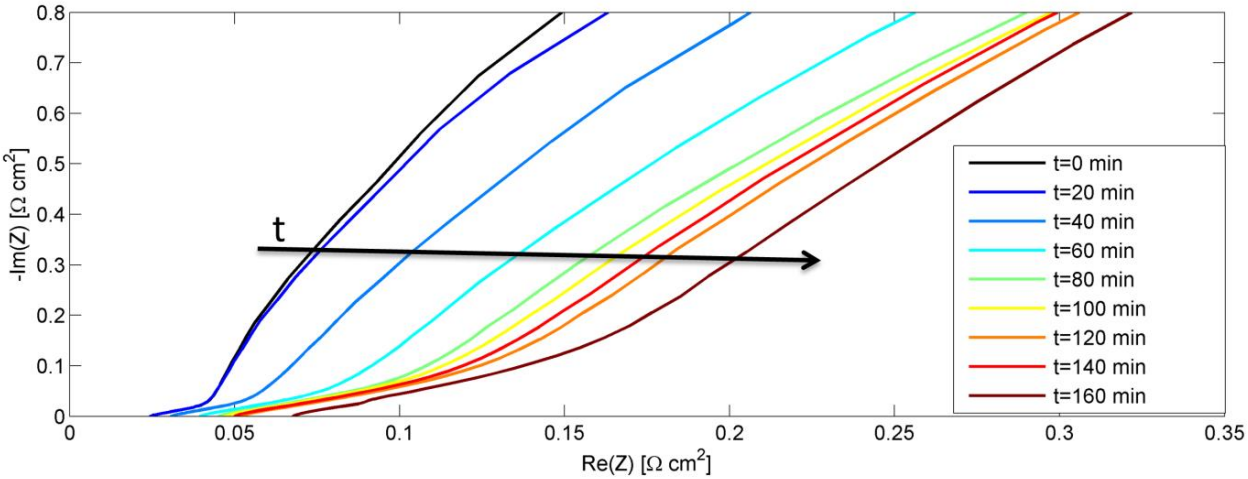

Figure 3.17: Electrochemical impedance spectroscopy during contamination with 200 ppm NH_3.

Figure 3.18 shows the EIS during the recovery when two CV cycles with scanning rate 50 mV/s and one EIS were performed every 10 minutes for five hours. The figure shows every third EIS measurement. After five hours recovery, the impedance is still higher than before NH_3 exposure.

Since the EIS is still improving between the last measurements, it is possible that the impedance is fully recovered if the recovery time is longer. It is not certain however that the recovery would be the same without a CV between each EIS measurement, since the CV affects the recovery process.

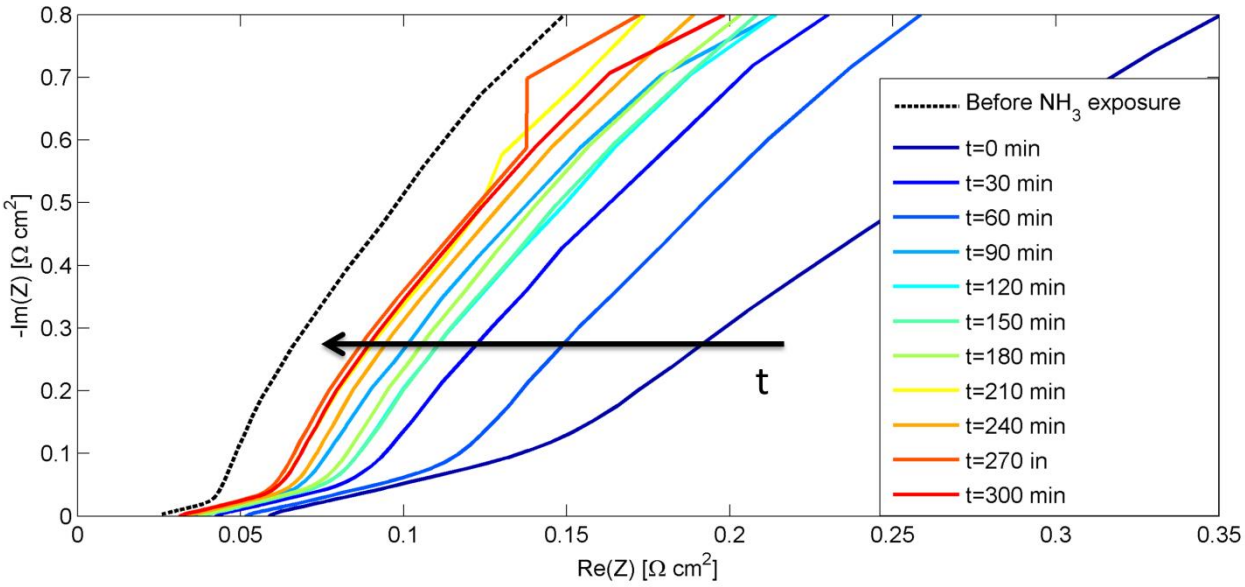

Figure3.18: EIS measurements performed after x minutes of recovery and EIS performed before 200 ppm NH3 exposure.

3.6.2 Polarization Curves and High Frequency Resistance

The hydrogen cross over was high in these experiments, partly because the hydrogen was not diluted with an inert gas. Figure 3.19 shows two polarization curves, one with the measured potential at different current densities and one where the potential is corrected for the overall cell resistance, including H_2 crossover.

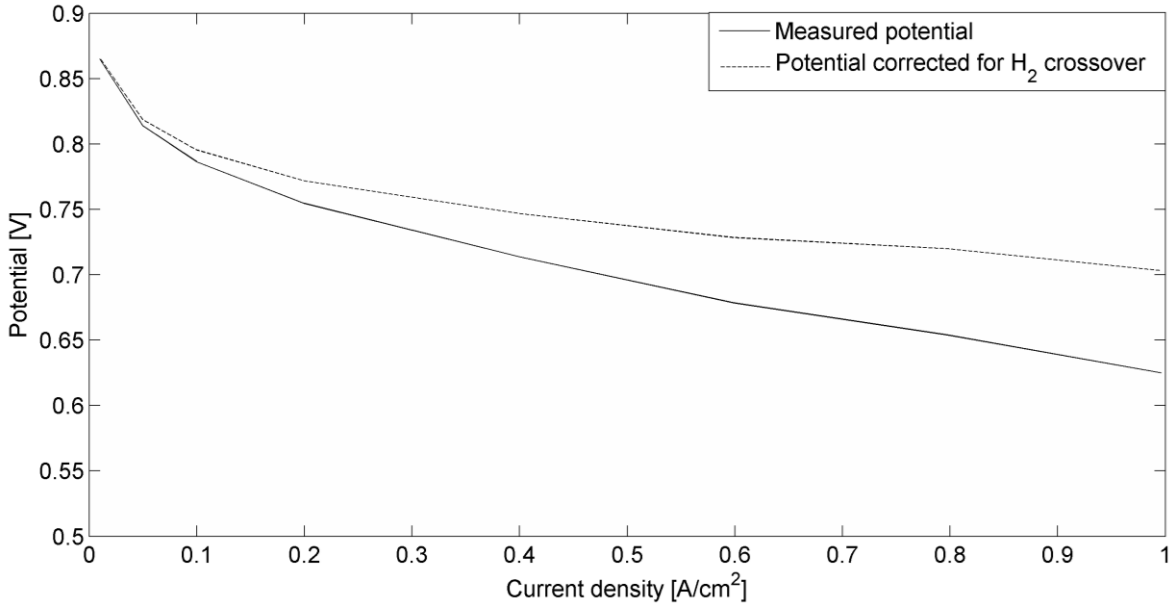

Figure 3.19: Polarization curve before NH_3 exposure with O_2 as cathode gas.

The corrected potential (E_{cor}) was calculated with eq 3.2, where Re(Z) is the real part of the impedance at 1 Hz.

$$E_{cor} = E_{measured} + I * area_{cell} * Re(Z) \quad [3.2]$$

The polarization curves in the following are not corrected for overall cell resistance.

Figure 3.20 shows the polarization curves for the experiment with 100 ppm NH_3 when oxygen was used as cathode gas. The polarization curve made during NH_3 exposure was in this and the other experiments made after the exposure time. The polarization curve made after recovery is above the one made before contamination. This means that the fuel cell performance has improved. The reason for this is probably that the activation process was not complete before the first polarization curve was made. Because of this improvement in the polarization curve, the conclusion that the fuel cell permanently degraded from NH_3 exposure, cannot be drawn. This was a reoccurring problem during the measurements with the test cells. The performance of the test cell improved from activation but it did also degrade when running for a longer time, which made it difficult to reach a steady state.

The polarization curve made during NH_3 exposure shows that the fuel cell performance has degraded during the contamination. At the current density of 0.5 A/cm^2, the potential has decreased from 0.74 V to 0.46 V.

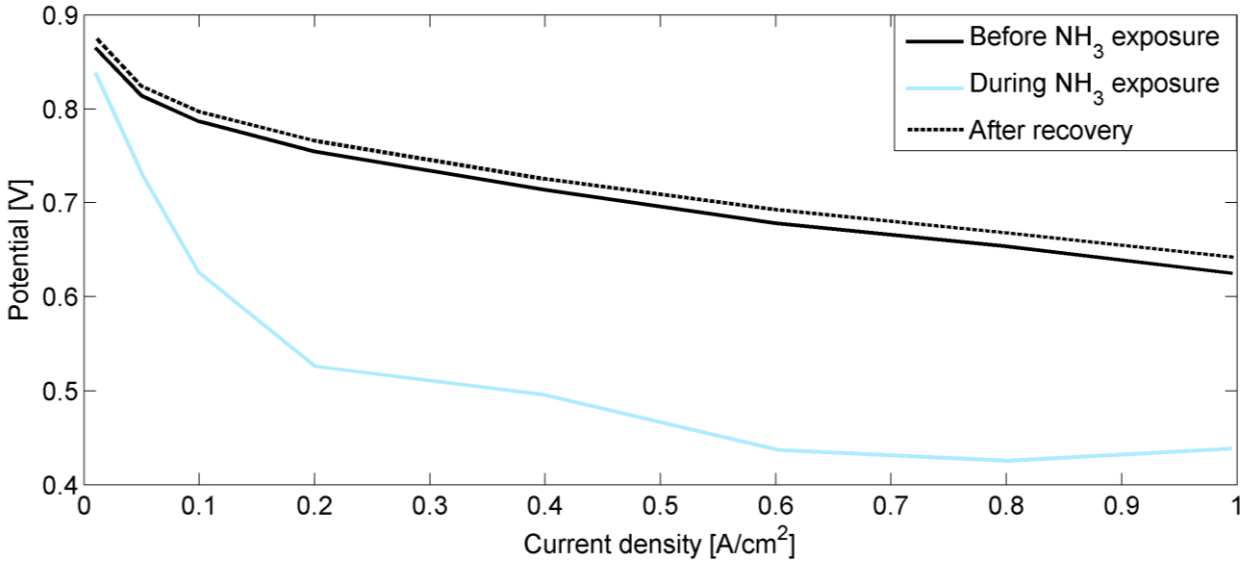

Figure 3.20: Polarization curve before and during 100 ppm NH3 exposure and after recovery with O_2 as cathode gas.

Figure 3.21 shows the polarization curves before contamination and during 200 ppm NH_3 exposure with oxygen and air as cathode gases. For current densities from 0.1 A/cm^2, the potential drop is about the same for both cathode gases.

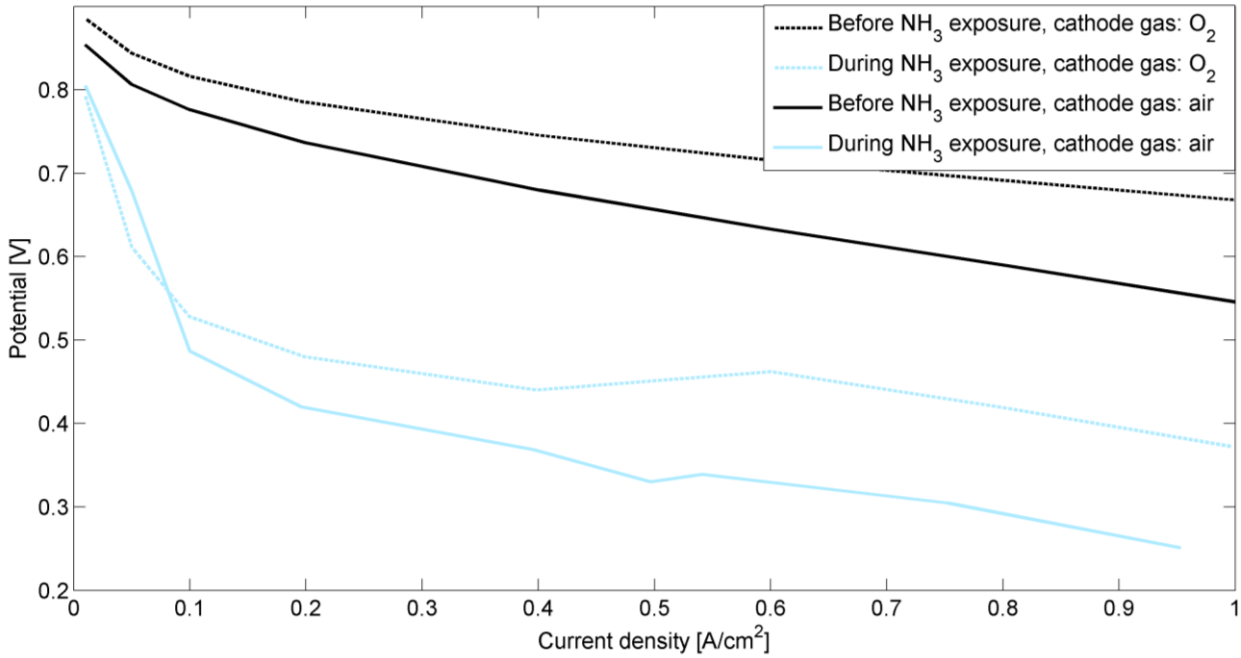

Figure 3.21: Polarization curve before and during 200 ppm NH3 exposure with O_2 and air as cathode gas respectively.

Figure 3.22 shows the potential during the HFR measurements with 200 ppm NH_3 with air (blue curve) and O_2 (black curve) used as cathode gases. The potential dropped from 0.72 V to 0.46 V during the contamination when oxygen was used as cathode gas and when air was used as cathode gas it dropped from 0.66 V to 0.37 V. The potential drop was thus slightly smaller when oxygen was used as cathode gas (0.26 V) compared to when air was used as cathode gas (0.29 V). This difference in voltage drop is small, especially when considering that the potential fluctuated ±0.01 V around the lower potential value. The recovery of the potential did not flatten out fully during the recovery time, which indicates that the potential might still rise to the original value, but it would take much more time. From this measurement and figure 3.21, it seems that the performance degradation of the fuel cell when exposed to NH_3 is the same when air and oxygen are used as cathode gases.

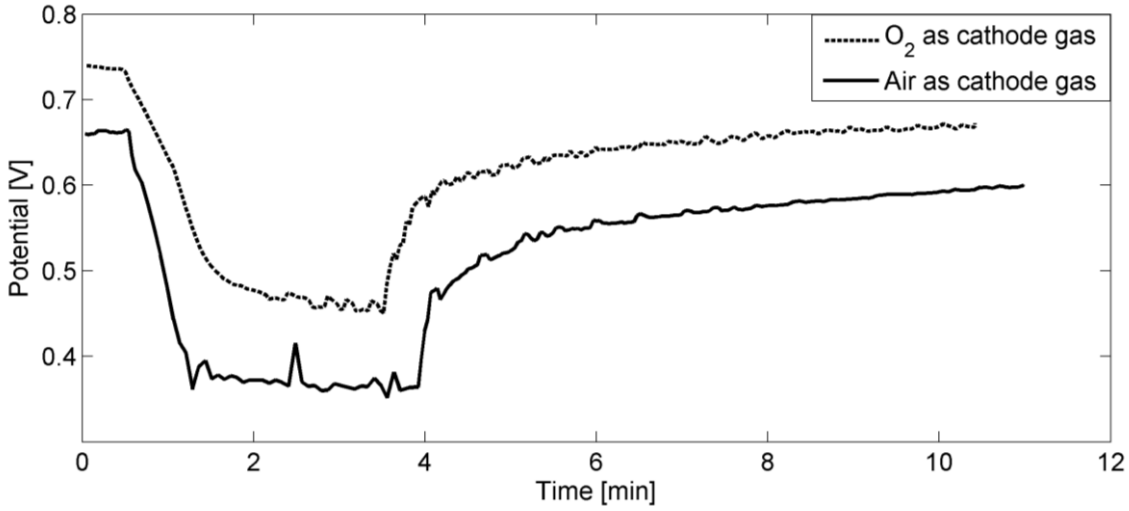

Figure 3.22: Potential from HFR measurements with 200 ppm NH_3.

Figure 3.23 shows the potential during the experiments with 100 ppm and 200 ppm NH_3. The cathode gas was in both cases O_2. Since the NH_3 exposure time was double for the experiment with 100 ppm compared to the experiment with 200 ppm, the total amount of NH_3 exposed to the cell was the same. In both cases the potential dropped fast at first and leveled then out. In the experiment with 200 ppm NH_3, the potential drop was 0.28 V and in the experiment with 100 ppm it was 0.24 V. The NH_3 poisoning of the fuel cell is thus not only dependent on the total amount of NH_3 exposed to the fuel cell, but also on the NH_3 concentration. The recovery was very similar for the two experiments and they seemed to reach the same final potential of around 0.68 V. The fuel cell thus seems to be irreversibly poisoned for both concentrations but full recovery might be possible with a longer recovery period.

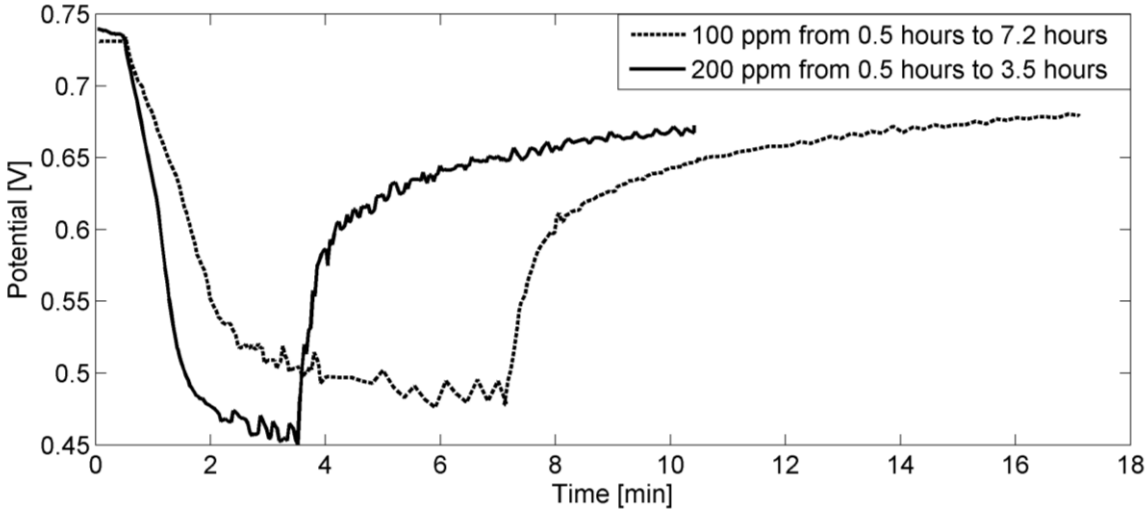

Figure 3.23: Potential during NH_3 contamination. Oxygen used as cathode gas.

From the experiments with NH_3 it is clear that both the cathode catalyst and the membrane are poisoned when the cell is exposed to 200 ppm. Zhang *et al.* [18] did also find that ammonia poisons both the membrane and the catalyst. They did CVs on the anode instead of the cathode, but since the diffusion of ammonia from the anode to the cathode is very fast [15], a similar result was expected. Regarding the reversibility, earlier works have shown that the effect of NH_3 can be both reversible and irreversible, depending on the NH_3 concentration and exposure time [13] [17]. In this work, high concentrations of NH_3 were used and the effect then seemed to be only partially reversible.

3.7 Propene

Figure 3.24 shows the potential during contamination with 100 ppm propene and with the constant current density of 0.5 A/cm^2. The black curve was made without air bleed and the red curve was made with 1 % air bleed. The first 30 minutes of the measurements were made without propene. The measurement made with air bleed starts out at a lower voltage, which could be due to the addition of air to the fuel, but it could also be a variation between the two MEAs. The voltage is decreasing similarly in the two measurements and the total potential drop after 20 hours exposure time is 8 mV for the measurement without air bleed and 6 mV for the measurement with air bleed. Figure 3.25 shows the polarization curves made after 20 hours propene exposure, with and without air bleed. There is virtually no difference between the two polarization curves.

The potential drop during the HFR measurements indicates that propene poisons the fuel cell when the current density is 0.5 A/cm^2, but it has to be verified with a measurement made in the same way but with the addition of pure argon instead of argon mixed with propene. That is to be sure that the potential drop is due to propene poisoning and not due to a decrease in fuel cell performance over time. The differences between the measurements made with propene are small and more measurements have to be made to conclude if air bleed affects the propene poisoning of the fuel cell.

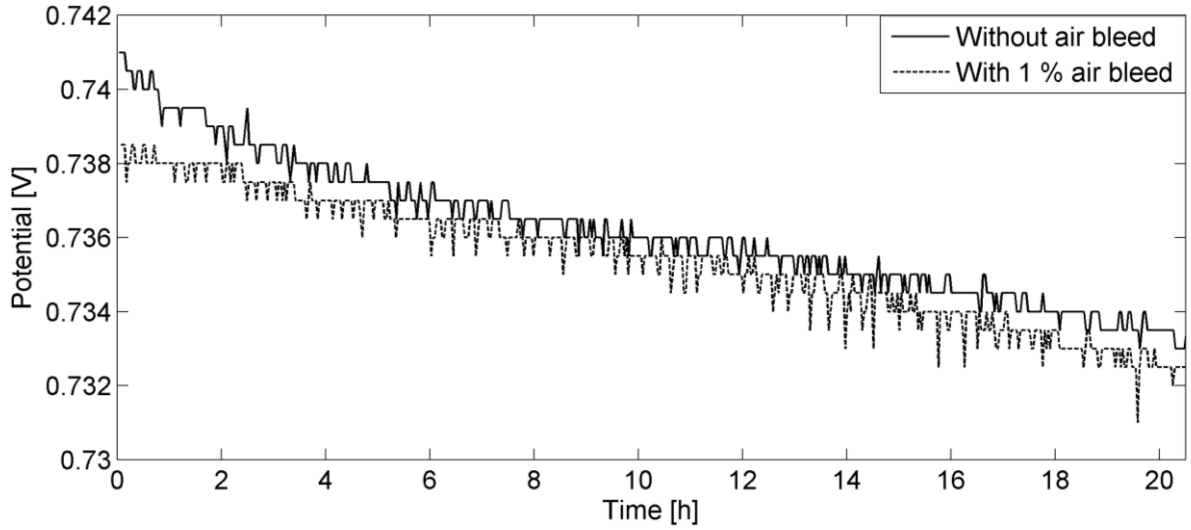

Figure 3.24: Potential from HFR measurements with 100 ppm propene.

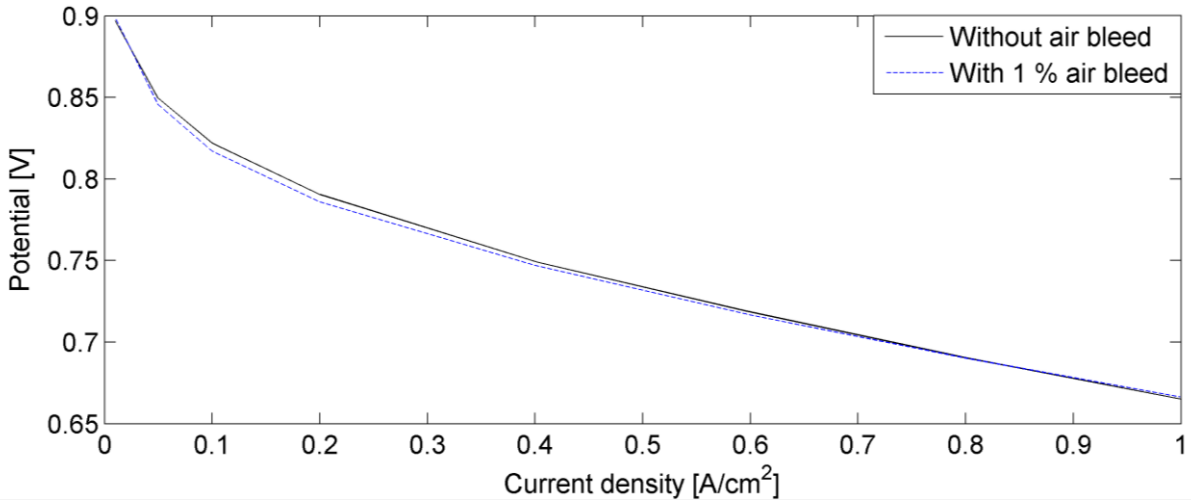

Figure 3.25: Polarization curves made after 20 hours exposure to 100 ppm propene.
Black curve: Without air bleed. Red curve: With 1 % air bleed.

3.8 Error sources

All experiments had some potential error sources in common, which might have affected the results. Those error sources were the following:

- Mass flow controller (MFC) fluctuations
- Temperature fluctuations
- Condensation in the fuel cells
- Problems with water transport inside the fuel cells

- Defects in the construction of the fuel cells. Both the test cell and the fuel cell stacks were put together manually. This means that the MEA and GDL might have been placed obliquely and all fuels cells might not have been pressed precisely even.

The fuel cell and the gas inlet tubes were insulated to avoid temperature fluctuations. This also helped to avoid condensation in the fuel cell. To further avoid condensation in the fuel cell, the cell temperature and the gas inlet temperatures were set to a higher value compared to the humidifiers. The gas flows were set to values known to be sufficient for a good water transport inside the fuel cell. To minimize the overall effect on the results of different potential errors, at least two measurements were made for each test.

Chapter 4

Conclusions and Future Work

The fuel cell tolerated CO levels up to 25 ppm with an air bleed of 0.5 %. The effect of CO poisoning of the fuel cell was mainly recoverable. However, after several tests with 50 ppm CO exposure, the voltage did not recover fully. Tests did not show whether it is possible to achieve the same CO tolerance with smaller amounts of air bleed by using pulsed air bleed.

For short time exposure (15 minutes), the fuel cell tolerates H_2S levels up to 10 ppm and SO_2 levels up to 20 ppm. When the fuel cell was exposed to 10 ppm of these sulfur contaminants for 4 hours, the performance degraded irreversibly. Consequently, if a problem occurs with the desulphurization of the anode gas and the fuel cell is exposed to 10 ppm of H_2S or SO_2, there will not be any performance degradation if the problem is fixed within 15 minutes, but if it is not fixed within 4 hours, the fuel cell will be permanently damaged. In future works it might be interesting to do the experiments with lower H_2S and SO_2 concentrations and longer exposure times. If the short time exposure experiments had been performed with a new MEA between each concentration, the results might have been different. This could also be done in a future work. Something else that could be done differently in future works is the recovery process. The recovery process after SO_2 exposure could be done with open circuit voltage to obtain maximum voltage. In this work, the lowest current density during recovery was 0.1 A/cm^2 which resulted in a voltage of 0.75 V. Oxidation peaks have been found at 0.89 and 1.05 V. To achieve 1.05 V, CV is necessary, but 0.89 V might be achievable with open circuit.

No poisoning of the fuel cell could be seen when ethylene and ethane were added to the fuel. Since the hydrocarbons were mixed with N_2 in tubes containing 1000 ppm ethylene/ethane, higher concentrations than 100 ppm could not be tested in a satisfying way. If the hydrocarbons had not been diluted in N_2, higher concentrations could have been tested.

When the fuel cell was exposed to 200 ppm NH_3, there was virtually no active catalyst area left on the cathode side after 80 minutes. After 3.5 hours recovery, the electro active catalyst area was still 30 % less than the original value. The fuel cell impedance increased during NH_3 exposure and it is not clear if it would recover fully when the NH_3 is removed from the fuel if the recovery time is longer than it was in this work. There was no difference in NH_3 poisoning of the fuel cell when the cathode gas was changed from oxygen to air. When the current density was held constant at 0.5 A/cm^2, the potential reached a steady state during the NH_3 exposure. This steady state potential was lower for higher NH_3 concentrations, which means that it is not only the total amount of NH_3 exposed to the fuel cell that affects the poisoning, but also the NH_3 concentration.

The measurements made with propene shows that 100 ppm propene mixed in the hydrogen gas does not poison the fuel cell severely when the exposure time is 20 hours. However, the measurements were not sufficient to conclude if the propene poisons the fuel cell at all and if air bleed affects the poisoning. More measurements have to be made with propene to draw these conclusions.

The results in this thesis are only valid for the conditions used in these experiments. Future works can therefore be made with different temperatures, humidities and potential during contamination. Since all these parameters, and more (like the MEA), affects the experiment, the results cannot be

compared in detail to results from other works, but the conclusions which can be drawn from the results in this thesis are basically the same as conclusions drawn in earlier cited works.

Bibliography

[1] J. Larminie and A. Dicks, Fuel cell systems explained, Chichester: John Wiley & Sons, 2003.

[2] N. Hikosaka Behling, Fuel Cells Current Technology Challenges and Future Research Needs, Amsterdam, Boston, Heidelberg, London, New York, Oxford, Paris, San Diego, San Fransisco, Singapore, Sydney, Tokyo: Elsevier, 2013.

[3] F. Barbir, PEM fuel cells: theory and practice, Storrs: Elsevier Academic Press, 2005.

[4] M. Matthew M, K. Emin Caglan and V. T. Nejat, Polymer electrolyte fuel cell degradation, Oxford: Academic Press, 2012.

[5] W. Shaohong, W. Jinfeng, Y. Xiao Zi, M. Jonathan J, W. Haijiang, Z. Jiujun, S. Jun and M. Walter, "A review of PEM fuel cell durability: Degradation mechanisms and mitigation strategies," vol. 184, no. 1, 2008.

[6] K. J. Mayrhofer, J. C. Meier, S. J. Ashton, G. K. Wiberg, F. Kraus, M. Hanzlik and M. Arenz, "Fuel cell catalyst degradation on the nanoscale," vol. 10, no. 8, 2008.

[7] X.-Z. Yuan, Electrochemical Impedance Spectroscopy in PEM Fuel Cells, New York: Springer, 2010.

[8] L. Hui, Proton exchange membrane fuel cells: contamination and mitigation strategies, Boca Raton: CRC Press, 2010.

[9] Southhampton Electrochemistry Group, INSTRUMENTAL METHODS IN ELECTROCHEMISTRY, Chichester: Horwood Publishing, 2001.

[10] C. Song, Y. Tang, J. L. Zhang, J. Zhang, H. Wang, J. Shen, S. McDermid, J. Li and P. Kozak, "ELECTROCHIMICA ACTA, PEM fuel cell reaction kinetics in the temperature range of 23–120 ◦C," vol. 52, no. 7, 2006.

[11] A. Baumann Ofstad, "Increasing the Lifetime of PEM Fuel Cells: A Characterization of some Degradation Mechanisms," Norwegian University of Science and Technology, Trondheim, 2010.

[12] T. Vidaković, M. Christov and K. Sundmacher, "The use of CO stripping for in situ fuel cell catalyst characterization," vol. 52, no. 18, 2007.

[13] X. Cheng, Z. Shi, N. Glass, L. Zhang, J. Zhang, D. Song, Z.-S. Liu, H. Wang and J. Shen, "A review of PEM hydrogen fuel cell contamination: Impacts, mechanisms, and mitigation," *Journal of Power Sources,* pp. 739-756, 2007.

[14] Z. Nada and L. Xianguo, "Effect of contaminants on polymer electrolyte membrane fuel cells," vol. 37, no. 3, 2011.

[15] R. Halseid, M. Heinen, Z. Jusys and R. J. Behm, "The effect of ammonium ions on oxygen reduction and hydrogen peroxide formation on polycrystalline Pt electrodes," vol. 176, no. 2, 2008.

[16] R. Halseid, P. J. Vie and R. Tunold, "Effect of ammonia on the performance of polymer electrolyte membrane fuel cells," vol. 154, no. 2, 2006.

[17] B. Rod, W. David, Z. Piotr, M. Karren, S. Ken, Z. Tom, B. James, M. James E, I. Minoru, M. Kenji, H. Michio, M. Jeremy, O. Kenichiro, O. Zempachi, M. Seizo and N. Atsushi, "Scientific aspects of polymer electrolyte fuel cell durability and degradation," *Chemical reviews,* vol. 107, no. 10, 2007.

[18] X. Zhang, U. Pasaogullari and T. Molter, "Influence of Ammonia on membrane-electrode assemblies in polymer electrolyte fuel cells," vol. 34, no. 22, 2009.

[19] K. Kortsdottir, R. Wreland Lindström and G. Lindbergh, "The influence of ethene impurities in the gas feed of a PEM fuel cell," vol. 38, no. 1, 2013.

[20] F. Javier Pérez Ferriz, "The influence of propene impurities on the PEM Fuel Cell catalyst," KTH Royal Institute of Technology, Stockholm, 2013.

[21] F. Jing, M. Hou, W. Shi, H. Yu, P. Ming and B. Yi, "The effect of ambient contamination on PEMFC performance," vol. 166, no. 1, 2007.

[22] Naturvårdsverket, "Miljömål," 21 Mars 2013. [Online]. Available: http://www.miljomal.se. [Accessed 9 10 2013].

[23] D. Yang, J. Ma, L. Xu, M. Wu and H. Wang, "The effect of nitrogen oxides in air on the performance of proton exchange membrane fuel cell," vol. 51, no. 19, 2006.

[24] R. Mothadi, W.-k. Lee and J. Van Zee, "Assessing durability of cathodes exposed to common air impurities," vol. 138, no. 1, 2004.

[25] B. Du, P. Richard, E. John F. and R. Manikandan, "Performance and Durability of a Polymer Electrolyte Fuel Cell Operating with Reformate: Effects of CO, CO2, and Other Trace Impurities," Springer Science + Business Media, Latham, 2009.

[26] T. Lopes, V. Paganin and E. Gonzalez, "The effects of hydrogen sulfide on the polymer electrolyte membrane fuel cell anode catalyst: H2S-Pt/C interaction products," vol. 196, no. 15, 2011.

[27] D. Papadias, S. Ahmed and R. Kumar, "Fuel Quality Issues in Stationary Fuek Cell Systems," Argonne National Laboratory, Agronne, 2011.

[28] X. Ma, D. Yang, W. Zhou, C. Zhang, X. Pan, L. Xu, M. Wu and J. Ma, "Evaluation of activated carbon adsorbent for fuel cell cathode air filtration," vol. 175, no. 1, 2007.

Appendix: Tables over experiments

Table 1: PowerCell Sweden AB

Contaminant	Concentration (ppm)	Exposure time (min)	Airbleed
CO	10	60	no
CO	10	60	0.5 % continuous
CO	25	60	no
CO	25	60	0.5 % continuous
CO	50	60	no
CO	50	60	0.5 % continuous
CO	50	60	1 % pulsed 10/10 s
CO	50	60	1 % pulsed 30/30 s
CO	50	60	2 % pulsed 10/30 s

Table 2: Volvo GTT/ATR

Contaminant	Concentration (ppm)	Exposure time (min)
C_2H_4	0.1	15
C_2H_4	1	15
C_2H_4	10	15
C_2H_4	100	15
C_2H_4	10	240
C_2H_6	0.1	15
C_2H_6	1	15
C_2H_6	10	15
C_2H_6	100	15
C_2H_6	10	240
H_2S	0.01	15
H_2S	0.1	15
H_2S	1	15
H_2S	5	15
H_2S	10	15
H_2S	20	15
H_2S	10	240
SO_2	0.05	15
SO_2	0.1	15
SO_2	1	15
SO_2	5	15
SO_2	10	15
SO_2	20	15
SO_2	30	15
SO_2	40	15
SO_2	10	240

Table 3: KTH

Concentration (ppm)	Exposure time (min)	Measurement before and during poisoning	Measurement during recovery	Cathode gas	Air bleed
200 NH_3	200	CV and EIS	CV	N_2	no
200 NH_3	200	CV and EIS	CV and EIS	N_2	no
200 NH_3	200	Potential during constant load and polarization curve	Potential during constant load and polarization curve	Air	no
200 NH_3	200	Potential during constant load and polarization curve	Potential during constant load and polarization curve	O_2	no
100 NH_3	400	Potential during constant load and polarization curve	Potential during constant load and polarization curve	O_2	no
100 C_3H_6	1200	Potential during constant load and polarization curve	No recovery measurement	O_2	no
100 C_3H_6	1200	Potential during constant load and polarization curve	No recovery measurement	O_2	1 %